Title

Time-lapse gravity monitoring of CO2 migration based on numerical modeling of a faulted storage complex

Authors
Appriou, Delphine
Bonneville, Alain
Zhou, Quanlin
et al.

Publication Date
2020-04-01

DOI
10.1016/j.ijggc.2020.102956

Peer reviewed

Time-Lapse Gravity Monitoring of CO_2 Migration Based on Numerical Modeling of a Faulted Storage Complex

Delphine Appriou[1], Alain Bonneville[1], Quanlin Zhou[2], and Erika Gasperikova[2]*

[1]Subsurface Science and Technology Group, Pacific Northwest National Laboratory PO Box 999. Richland, WA 99352, USA

[2]Energy Geosciences Division, Lawrence Berkeley National Laboratory, Berkeley, CA 94720, USA

[*]Corresponding author: Pacific Northwest National Laboratory, 902 Battelle Boulevard,
15 P.O. Box 999, Richland, WA 99352, Phone: (509) 375-4541, E-mail: Delphine.Appriou@pnnl.gov

Conflict of interest: None

Key words: Time-lapse gravity monitoring, leak detection, Geologic CO_2 storage, Kimberlina, CCS

Abstract

In this study, the performance of both surface and borehole time-lapse gravity monitoring to detect CO_2 leakage from a carbon storage site is evaluated. Several hypothetical scenarios of CO_2 migration in a leaky fault, and thief zones at different depths at the Kimberlina site (California, USA) constitute the basis of the approach. The CO_2 displacement is simulated using the TOUGH2 simulator applied to a detailed geological model of the site. The gravity responses to these CO_2 plumes are simulated using forward modeling with sensors at ground surface and in vertical boreholes. Results of inversion on one scenario are also presented. The surface-based gravity responses obtained for the different leakage scenarios demonstrate that leakage can be detected at the surface in all the scenarios but the time to detection is highly variable (10 to 40 years) and dependent on the detection threshold considered. Borehole measurements of the vertical component of gravity provide excellent constraints in depth when they are located in proximity of the density anomaly associated with the presence of CO_2, thus discriminating multiple leaks in different thief zones. Joint inversion of surface and borehole data can bring valuable information of the occurrence of leakages and their importance by providing a reasonable estimate of mass of displaced fluids. This study demonstrates the importance of combining multiphase flow simulations with gravity modeling in order to define if and when gravity monitoring would be applicable at a given storage site.

1. Introduction

Leakage of CO_2 from storage reservoirs has been identified in previous studies as one of the potential obstacles to large-scale Carbon Capture and Storage (CCS) deployment (Hepple and Benson, 2005; Herzog, 2011). Impacts of unexpected CO_2 migration into groundwater resources (Birkholzer et al., 2009; Keating et al., 2013; Kim et al., 2018; Lions et al., 2014), risk management (Anderson, 2017; White and Foxall, 2016), economic issues and liability of CO_2 leakage (Bielicki et al., 2016; Bielicki et al., 2014; Pollak et al., 2013) are all topics related to CO_2 leakage discussed in the recent literature. The ability to detect and quantify these potential leaks using geophysical or geochemical monitoring methods remains nonetheless challenging. Continuous advancements in instrumentations have demonstrated that time-lapse gravity is a viable method for effective reservoir monitoring but only a limited number of studies focus on the feasibility and effectiveness of this method to detect unforeseen upward CO_2 migration out of the reservoir. This study is motivated by the need to understand the limits and expectations of the method for leak detection, and ultimately to understand requirements, both spatial and temporal, for time-lapse gravity surveys design for efficient monitoring of leakage.

The concern of CO_2 leakage out of a reservoir is intrinsically related to CO_2 properties. Due to CO_2 buoyancy, any manmade or natural pathways can lead to upward migration of CO_2 and potentially a loss of CO_2 containment in a storage complex (IPCC, 2005). Preferential leakage pathways may therefore include poorly plugged wellbores (Jordan et al., 2015), or permeable structural features, such as geological faults or fractures (Lewicki et al., 2006). Because hydraulic properties of those leakage pathways may change with time in response to changes in rock stress, fluid pressure or fluid temperature (Nicol et al., 2017), CO_2 migration may occur during or after the injection phase of a project. The risks associated with CO_2 leakage include accumulation of CO_2 in overlying geological formations with a potential deterioration of groundwater resources (Keating et al., 2010; Lawter et al., 2016; Yang et al., 2014a; Yang et al., 2014b) or interference with other subsurface activities (Bielicki et al., 2014). If not partially diverted sideways into intermediate aquifers in “secondary trappings” (Bielicki et al., 2016), the upward migrating CO_2 could eventually be discharged to the atmosphere, resulting in a failure in reducing greenhouse gas emissions, and potentially present hazards to human health and the environment (Anderson, 2017; Deng et al., 2017).

CO_2 injection in a storage complex and CO_2 and brine leakage drive changes in subsurface properties, including changes in pressure, CO_2 saturation, pH, or total dissolved solids. A broad range technologies can be deployed at storage sites to track these changes (Chadwick et al., 2009; Furre et al., 2017; Hannis et al., 2017; Harbert et al., 2016) with three primary monitoring objectives: containment assurance, conformance assurance and contingency monitoring. The role of containment monitoring is to demonstrate that injected CO_2 is effectively and safely contained within the storage complex during and long after the injection phase of the project and must provide accurate estimates of the mass of CO_2 stored. Conformance monitoring is intended to compare the forecast from modeling to the observed behavior of CO_2 in the storage complex. This comparison is used for calibration and prediction with the aim of demonstrating that the long-term predictions are valid. A third category of monitoring, contingency monitoring, is required in the event of observations from the existing monitoring network that indicate that the storage complex has failed, leading to CO_2 migration through the overburden and potentially into the atmosphere or the ocean for offshore carbon storage reservoirs. Compliance to these CO_2 storage performance criteria is captured in regulatory and policy frameworks (e.g., European Union CCS Directive, 2009; U.S. EPA, 2010) and seeks to minimize the risk of leakage from the storage complex and to quantify and mitigate any unforeseen leaks that arise.

Several studies related to the evaluation of monitoring technologies for CO_2 leakage focused on monitoring technologies at the surface or in the shallow subsurface, such as soil-gas, atmospheric, microbiology monitoring, fluid pressure measurements or geochemical sampling (Romanak et al., 2012). Any unforeseen signals from these monitoring techniques would indicate that CO_2 has reached or is about to reach the surface. Although near-surface monitoring is essential for public acceptance, liability, and accounting purposes (Feitz et al., 2014), early detection of CO_2 migration from the storage reservoir is critical for contingency actions in order to avoid potential adverse impacts.

Several studies have focused on the feasibility of leak detection by monitoring for pressure changes in permeable aquifers overlying the storage reservoir (Chabora and Benson, 2009; Jung et al., 2013, 2015; Namhata et al., 2017). These studies have demonstrated the effectiveness of downhole monitoring of pressure changes to detect unexpected migration of CO_2 out of the reservoir; however an important limitation of the method relies on the fact that pressure measurements are point measurements by definition, limiting therefore the volume of investigation. Conversely, deep-subsurface geophysical monitoring technologies, such as 3D seismic or time-lapse gravity, allow the investigation of a large volume in the subsurface. They have been primarily used for tracking CO_2 migration in the storage reservoir to understand reservoir dynamics and therefore help predict future behavior. It is still a challenge for these deep-subsurface monitoring technologies to reliably detect changes at a satisfactory resolution in the overburden that can indicate CO_2 movement out of the storage reservoir. Wang et al. (2018) showed that the reduction in noise levels of seismic data is critical to detect supercritical CO_2 leakage in a deep formation. Similarly, numerical studies successfully demonstrated that surface gravity surveys are well adapted for detecting the bulk of the CO_2 plume in the storage reservoir (Gasperikova and Hoversten, 2008; Jacob et al., 2016; Krahenbuhl et al., 2011), but are not suitable to reveal small-to-moderate CO_2 accumulations associated with leakage (Jacob et al., 2016).

To demonstrate the ability of the gravity monitoring method to detect CO_2 leaks from a storage complex, several hypothetical scenarios of CO_2 injection in a storage reservoir and migration along a leaky fault into thief zones at different depths at the Kimberlina site (California, USA) have been developed for the present study. The CO_2 migration is simulated using the TOUGH2-MP/ECO2N simulator (Pruess, 2004; Zhang et al., 2008), based on a detailed geological model (Wagoner, 2009) and the rock properties presented in the papers by Zhou and Birkholzer (2011) and Wainwright et al. (2013). The responses of gravity to these CO_2 plumes are simulated using a forward modeling approach with instrumentation at ground surface and in vertical boreholes. Results of inversion on one scenario are also presented to illustrate the potential of the method in estimating the mass of leaked CO_2.

2. Gravity method: A well-known and still promising method

2.1 Monitoring of CCS site with time-lapse gravity surveys

Injection of CO_2 in a reservoir induces fluid displacement and changes in saturation that lead to a mass redistribution in the subsurface. Because the Earth's gravitational field is directly related to the mass distribution, repeated gravity surveys can be used to monitor mass balance changes over time and, in the case of carbon storage, fluid migration in the subsurface associated with CO_2 injection. The technique consists of measuring the downward acceleration of gravity (g_z) at a series of specific locations using high-precision gravimeters and repeating the measurements at defined times, with the aim of assessing the changes in gravity between measurements. Gravity measurements are made either at the ground surface or in boreholes.

Land-based gravity surveys can commonly achieve micro-Gal (μGal) accuracy with measurements repeatability as low as 3 μGal (Krahenbuhl et al., 2011; Van Camp et al., 2017). Borehole gravimeters like Gravilog™ (Nind et al., 2013) can operate in small diameter boreholes that deviate from vertical by up to ~60°. Emerging three-axis microgravity technology microelectromechanical system (MEMS) gravimeter and subsequent modeling studies indicate that valuable direction/azimuthal information could also be recovered for reservoir surveillance although no actual field experiment has been implemented (Lofts et al., 2019). As highlighted in Krahenbuhl and Li (2012), these continuous advancements in both applications and in instrumentation demonstrate that the gravity method is transitioning from a traditional exploration tool to a reservoir management and monitoring tool, including for carbon storage.

For instance, a comprehensive acquisition of gravity measurements to monitor gas production and CO_2 injection as part of a time-lapse gravity strategy occurred in 2002, on the offshore site of Sleipner in the Norwegian North Sea (Nooner et al., 2007). This initial survey was followed by repeat surveys in 2005, 2009 and 2013 (Alnes et al., 2011; Furre et al., 2017). Although the implementation of gravity surveys offshore was technically challenging (e.g., noise, establishing a benchmark height, etc.), the interpretation of time-lapse gravity data in combination with seismic data provided a unique dataset, leading to the determination of CO_2 density and supporting the notion that the gravity method is well suited for conformance monitoring. The first time-lapse gravity survey using a borehole gravimeter applied to a CO_2 storage site was conducted at the Cranfield site, Mississippi, as part of the Southeast Partnership test (Dodds, et al., 2013). The results showed a significant decrease in density contrast following the injection, consistent with the CO_2 locations predicted from reservoir simulations.

Fabriol et al. (2011), Gasperikova and Hoversten (2008), Jacob et al. (2016), and Krahenbuhl et al. (2011) numerically assessed the performance of the gravity method for monitoring carbon storage sites and discussed the benefits and limitations of using time-lapse gravity surveys. Benefits include the possibility to recover, relatively easily, the mass of stored CO_2 at a cost that is much less than cost-prohibitive seismic methods. Limitations include the inadequately low depth resolution for surface surveys, the limited density contrast that may exist in some formations due to the presence of multiple fluids (e.g., Sleipner), or due to the depth of injection. More recently, Wilkinson et al. (2017) also using a numerical modeling approach, demonstrated that a gravity anomaly due to leakage from a deep reservoir could be detected from the surface provided that there is an accumulation of CO_2 in a shallow aquifer.

Additionally, gravity being by essence sensitive to the mass distribution in the subsurface, any natural or manmade phenomena leading to a redistribution of mass contributes to the overall gravity response observed during time-lapse gravity surveys. The discrimination between other sources contributing to the gravity response at ground surface, such as seasonal or long-term temporal changes in groundwater mass, or the elevation changes at the survey stations, must also be taken into considerations. The contribution from the near-surface hydrologic phenomena are highly variable and site-specific but they can be spatially correlated and controlled by topography (Hare et al., 1999) and can be filtered or numerical modeling of their effects can be attempted. The variation of stations elevation between two consecutive surveys is another source of important gravity anomaly because the elevation of the instrument affects gravity measurements (0.3086 mGal/m). At large scale these variations can be either positive (uplift) due for example to the poroelastic effect of CO_2 plume emplaced at shallow depth or negative (subsidence) like the one induced by groundwater pumping being faster than aquifer recharge. All these effects can be corrected by measuring accurately the elevation at each gravity station using differential Ground Positioning System (DGPS) which provides vertical position accuracy at the centimeter level (equivalent to a 3 μGal accuracy for the gravity measurement).

2.2 Density contrast: Key parameter of time-lapse gravity monitoring

The performance of the gravity method applied at CCS sites relies on the density contrast observed over time and associated with the injection of CO_2 that displaces initial fluids. The density of CO_2 varies significantly with pressure and temperature. At atmospheric conditions, CO_2 is a low-density gas. Under typical operational conditions encountered at CS sites, CO_2 is injected as a liquid and reaches a supercritical state at pressures greater than 7.39 MPa and temperatures higher than 31.1 °C. These conditions are generally met at a depth greater than 800 m but the exact depth is variable and directly related to the geothermal and pore pressure gradient existing at a given site. Because CO_2 is less dense than the in-situ fluids, CO_2 injection results in a bulk density decrease over time, as CO_2 partially or totally displaces brine in the pore space. In the event of the existence of a pathway in the impermeable cap rock (e.g., leaky wells, fractures, etc.), buoyant CO_2 migrates to the shallower formations, and may undergo a phase transition from supercritical phase to gaseous phase (Figure 1). When buoyed to shallow formations, its density will significantly decrease, and its volume become much larger. These property changes are the key for considering time-lapse gravity surveys as a valuable monitoring tool with increased likelihood of detecting large volumes of low-density fluid approaching the surface.

The goal of time-lapse gravity monitoring at storage sites is to determine temporal gravity anomalies related to the injection of CO_2 and exclusively associated with the redistribution of fluids (i.e., CO_2 and brine) in the pore space. Gravity measurements are performed exactly at the same spatial positions in each individual survey. Corrections typically depending on the location at the surface of the Earth remain constant over time and *ipso facto* accounted in time-lapse processing (Davis et al., 2008). Assuming that porosity changes are negligible over time, the bulk density change $\Delta\rho$ between two time steps within a saline formation, such as the Vedder sandstone considered for the simulations at the Kimberlina site (see section 3), is only dependent on the change in fluid density (i.e., CO_2 and brine) and can be expressed as:

$$\Delta\rho = \Delta \mathrm{S}_{\mathrm{CO_2}} \phi \left(\rho_{CO_2} - \rho_{brine}\right) \quad (1)$$

where $\Delta \mathrm{S}_{\mathrm{CO_2}}$ is the change in CO_2 saturation, ϕ is the porosity, ρ_{CO_2} is the CO_2 density and ρ_{brine} is the brine density (Eiken et al., 2008; Jacob et al., 2016). This density change directly influences gravity variations. As stated previously, equation 1 is based on the assumption that porosity changes caused by CO_2 injection are negligible. Kabirzadeh et al. (2017) studied the effect of porosity variations in the reservoir and their impact on the gravity response, but unless important deformations of the ground surface are observed (on the order of tens of centimeters), this effect seems to be very limited. As other potential field methods, gravity is inversely proportional to the square of the distance between the source and the observation station. Downhole gravity measurements being closer to the sources present a signal larger than at the surface and can potentially detect much smaller changes in the subsurface mass distribution than surface measurements.

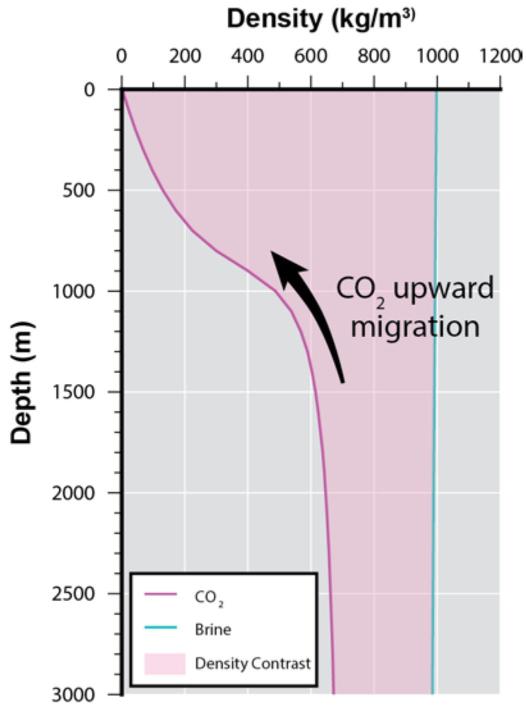

Figure 1. Brine Density (blue) and CO_2 density (pink) as a function of depth at the Kimberlina site. Geothermal gradient is 26.8 ℃/km, average surface temperature is 21.8 ℃. The salinity gradient is very low at 6.7 ppm/m and geothermal gradient is high, which explains why the density of brine slightly decreases with depth. Colored area represents the increasing density contrast as depth decreases, enhancing the potential for detection of leakage using the gravity method.

3. Modeling CO_2 injection and leakage at Kimberlina

3.1 Geological setting

The performance of time-lapse gravity monitoring is evaluated for a number of CO_2 leakage scenarios developed on a hypothetical reservoir-scale model initially established for the Kimberlina storage complex (Zhou and Birkholzer, 2011). The Kimberlina site is located in the southern San Joaquin Valley in California between the Sierra Nevada Mountains to the east and the Coast Ranges to the west (Figure 2). The southern part of the San Joaquin Valley is filled by more than 7000 m of Tertiary marine and non-marine sediments. The targeted storage formation is the Vedder Formation, a large permeable sandstone formed by marine and coastal marine sediments. Other permeable formations include the Olcese Formation, the Santa Margarita Formation and the Etchegoin Formation, which are three sandstone formations located above the reservoir. Several thick sealing shale units overlie the Vedder Formation, including the Freeman-Fruitvale shale, the Round Mountain shale and the Macoma shale. The stratigraphy was thus considered of particular interest to safe storage of large quantities of CO_2. This is counterbalanced by the existence of numerous faults in this part of the basin, such as the Pond-Poso-Creek fault zone, which adds structural complexities and operational risks as CO_2 migrates through the reservoir. The Pond-Poso Creek fault zone is part of a northwesterly-striking normal faulting system, dipping to the southwest at 50 to 70 degrees (Wagoner, 2009). This area also includes numerous wells, and well leakage is also a risk at this site but this possible leakage pathway is beyond the scope of this paper.

Based on the initial large geological model and flow model developed by Zhou and Birkholzer, (2011), a 25-layer submodel (38 km × 38 km), referred to as the Kimberlina 2 model, was developed for this study with a focus on the Vedder Sandstone near the Pond-Poso-Creek fault. The Vedder top updips northeast at 7°. The model was rotated so that the northern part of the fault aligns with X-Y direction. The Kimberlina

2 model was then used to simulate CO_2 storage in the Vedder Sandstone and hypothetical scenarios of subsequent leakage through the fault into the three permeable sandstone formations identified above and referred to now as thief zones (Figure 3). These simulated three dimensions (3D) CO_2 plumes were then used to calculate the vertical component of gravity.

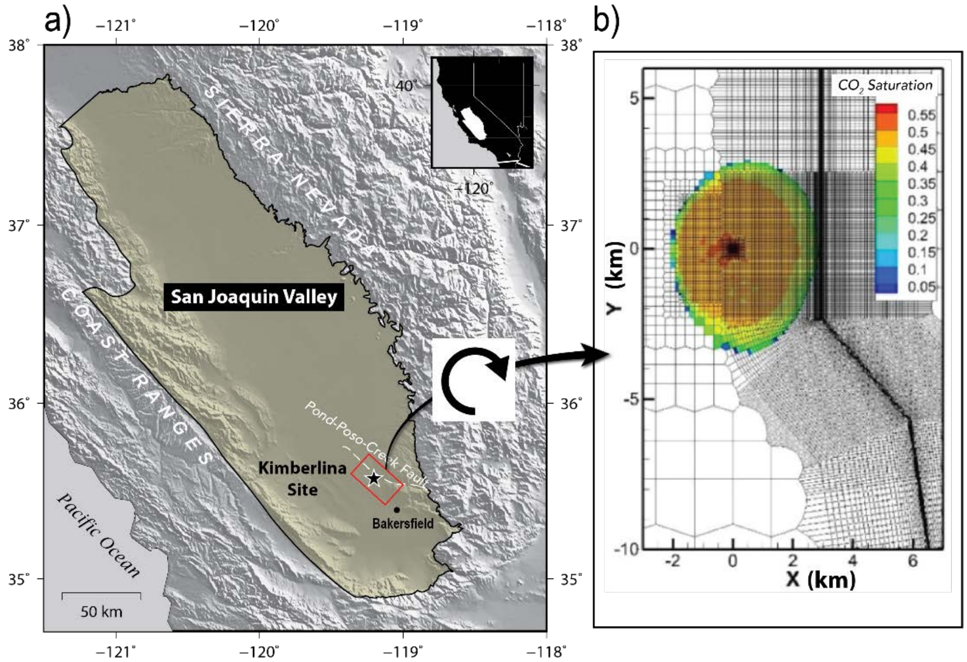

Figure 2. Location of the Kimberlina Project in the San Joaquin Valley (a). The Pond-Poso-Creek fault System bounds the storage complex on the east. (b) The model was rotated and subsequently used to conduct fluid flow simulations with TOUGH2-MP. The CO_2 saturation 40 years after the beginning of the injection is shown.

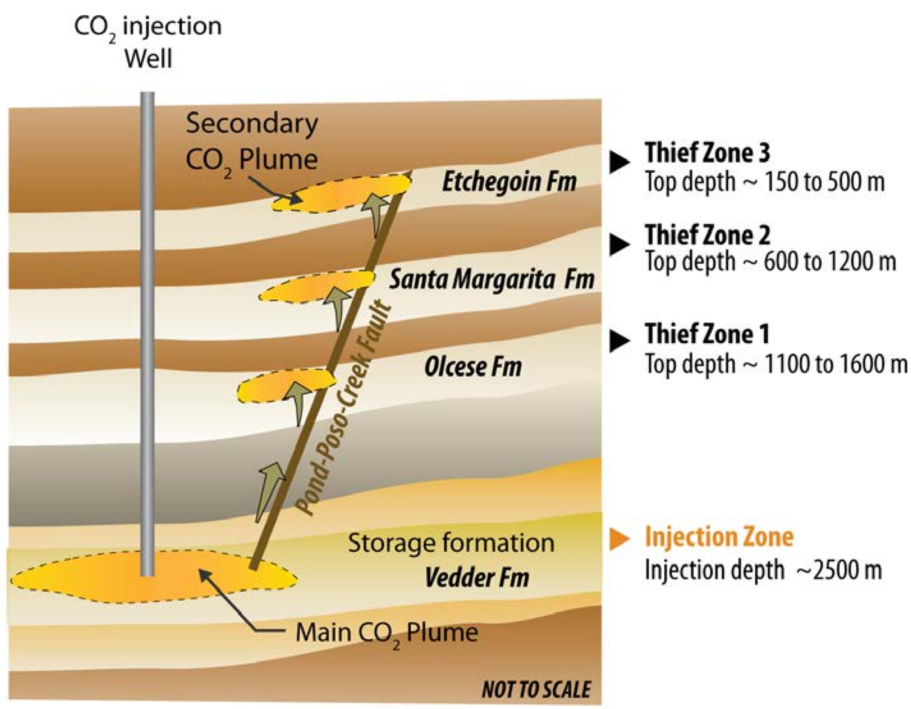

Figure 3. Conceptual cross-section of the southern part of the San Joaquin Valley showing potential CO_2 leakage pathways modeled in the hypothetical scenarios. The scenarios used for the simulations consist of CO_2 injection into the injection zone and CO_2 leaked through the Pond-Poso-Creek fault into up to three thief zones: Olcese Formation (thief zone 1), Santa Margarita Formation (thief zone2), and Etchegoin Formation (thief zone 3). These formations are dipping and thus depth ranges are given instead of single values.

3.2 Model parameters

The injection of CO_2 into the deep Vedder Formation was simulated at a rate of 2.5 million metric tons (Mt) of CO_2 per year for 60 years, followed by a 140-year post-injection monitoring period. All the fluid flow simulations were performed with TOUGH2-MP/ECO2N, the massively parallel version of the TOUGH2 code (Zhang et al., 2008) to predict the dynamic CO_2 storage in the subsurface.The initial conditions were set with linear geothermal, pore pressure and salinity gradients (26.8 °C/km, 10.5 MPa/km and 6.7 ppm/m, respectively). Dissolution of CO_2 into brine is taken into account until 70 years but, due to problems of convergence of the solutions at the front of the plume for the various leakage scenarios, it was not considered for time greater than 70 years. It must be noted though that the dissolution rate being very moderated after 70 years, this doesn’t impact the results in terms of quantification of the CO_2 free gaseous phase. Table 1 provides additional information about the main parameters used to develop the Kimberlina 2 multi-phase flow model.

Table 1. Parameters used for the Kimberlina 2 model simulations

Model Parameters	
Model dimensions	38 km × 38 km / 25 layers
Number of elements	2 562 357
Study area	12.5 km × 16 km × 3 km
Initial Conditions	
Surface temperature	21.8 °C
Geothermal gradient	26.8 °C/km
Salinity Gradient	6.7 ppm/m
Hydrostatic Pressure Gradient	10.5 MPa/km
Reservoir Parameters	
Reservoir	Vedder Sandstone
Injection zone depth	~ 2500 m
Reservoir depth	1600 to 3000 m
Reservoir thickness	50 m
Reservoir porosity	26 %
Reservoir permeability	Kx = Ky = 307 mD, Kz = Kx × 0.2
Injection Parameters	
Well Location	x = 0, y = 0
CO_2 injection rate	2.5 Mt/yr
Injection duration	60 yr
Post-injection duration	140 yr
Total injected CO_2 volume	150 Mt
Thief Zones Parameters	
Olcese permeability	Kx = Ky = 170 mD, Kz = Kx × 0.1
Olcese porosity	33.6 %
Santa Margarita permeability	Kx = Ky = 200 mD, Kz = Kx × 0.1
Santa Margarita porosity	27.5 %
Etchegoin permeability	Kx = Ky = 120 mD, Kz = Kx × 0.1
Etchegoin porosity	32 %

3.3 Leakage scenarios

To perform the assessment of the gravity method for CO_2 leakage detection, the study area focuses on the injection point and the fault, which represents a 12.5 km by 16 km area. A first set of simulations was designed to track CO_2 plume evolution in the storage formation while the Pond-Poso-Creek fault remains sealing (baseline scenario). Then, changes in the fault permeability through leaky windows were introduced, assuming leakage into up to three thief zones. Only a section of the fault is conductive while the remainder remains sealing. These conductive sections, or windows, are either termed “Location 1” or “Location 2”. For each leakage scenario, the changes in the fault permeability occurred at 70 years, 10 years after the end of the injection. The deepest thief zone considered in these scenarios is the Olcese formation, lying between 1100 and 1600 m deep (due to steeply dipping strata). The middle thief zone, the Santa Margarita formation, lies between 600 and 1200 m and the shallowest thief zone, the Etchegoin formation, is located between 150 and 500 m below the ground surface (Figure 3).

A total of 7 leakage scenarios are evaluated. The first set of leakage scenarios is for location 1, located 2.9 km east from the injection well (Figure 4). The scenarios studied include CO_2 migration into either Olcene or Etchegoin formations or both (Table 2). The sealing formations above the secondary leak are intact, hence no CO_2 comes to the surface. The second set of leakage scenarios is for location 2 located 6 km southeast of the injection well (Figure 4). This set includes secondary CO_2 accumulations in one of the three thief zones (Olcese, Santa Margarita or Etchegoin), and in three thief zones simultaneously (Table 2). The masses of leakage considered in these scenarios could seem large (e.g., over 12 Mt of leaked CO_2 after 130 years of leakage in the Olcese Formation); however, these scenarios are hypothetical and are being evaluated to assess the effectiveness of gravity monitoring to detection CO_2 into overlying thief zones.

For each leakage scenario evaluated in this study, the time-dependent CO_2 mass leaked into these zones is plotted in Figure 5, along with the minimum depth reached by the CO_2. The total CO_2 mass leaked in each thief zone differs. At both leakage locations, a total of over 12 Mt of CO_2 leaks into the Olcese Formation, the deepest thief zone. At the locations 1 and 2, about 4 Mt of CO_2 leaked into the Etchegoin Formation, the shallowest thief zone. At the location 2, one scenario considers a leakage of more than 10 Mt of CO_2 into the Santa Margarita Formation, the intermediate thief zone. Two scenarios consider simultaneous leakage. At the location 1, Etchegoin and Olcese formations are the two thief zones active for leaked CO_2 to migrate into, with respective total CO_2 mass leaked of 3.5 and 9.1 Mt. At the location 2, a scenario considered the three thief zones as being simultaneously active with a CO_2 mass leaked of 4.1 Mt in the Olcese formation, 5.4 Mt in the Santa Margarita formation and 4.2 Mt in the Etchegoin formation (Table 2). Although CO_2 upward migration is initiated at 70 years for all leakage scenarios, the actual time of arrival of the CO_2 into the respective thief zone(s) is highly dependent on the depth of these leakage intervals. For instance, Figure 5 shows that CO_2 reaches the Olcese and the Santa Maragarita thief zones only 2 to 5 years after the beginning of the leak while CO_2 is reaching the shallowest thief zone (i.e., Etchegoin formation), at 100 years, 30 years after the leak was initiated. The mechanism leading to the different time of arrival of the CO_2 into the thief zones is not critical for this study; however, knowing if the gravity method could detect it when CO_2 enters the thief zones is key.

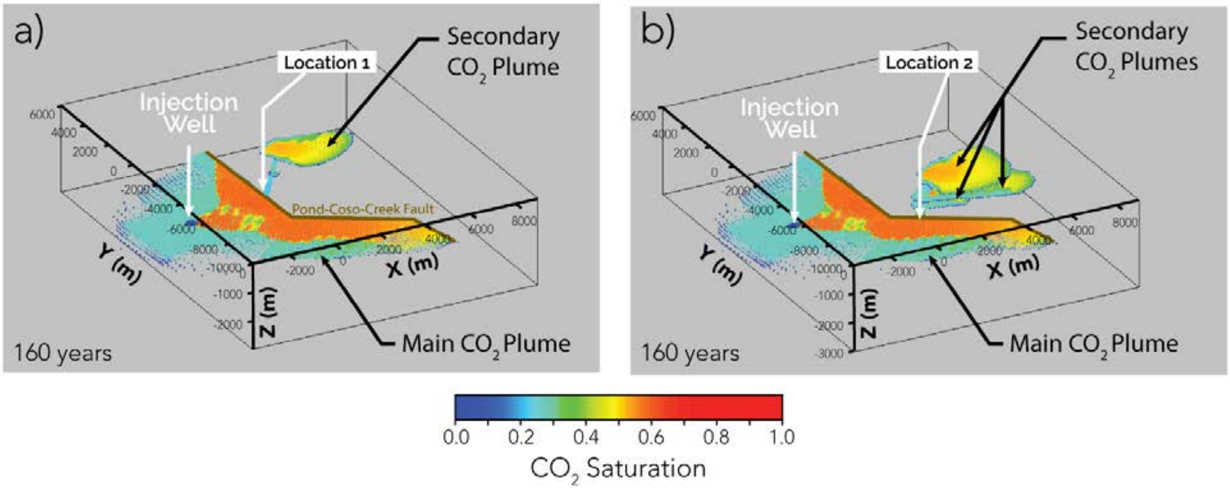

Figure 4. a) CO_2 saturation at 160 years resulting from a leak occurring at location 1 in the Etchegoin formation. b) CO_2 saturation at 160 years resulting from a leakage occurring at location 2 in the three thief zones

Table 2. Leakage scenarios with thief zones active for leaked CO_2 to migrate into with respective total leaked CO_2 mass in Mt.

Total leaked CO_2 mass (Mt) entering the thief zones				
Scenario	**#**	**Olcese (OL)**	**Santa Margarita (SM)**	**Etchegoin (ET)**
Baseline	0	-	-	-
Location 1				
OL	1.1	12.6		
ET	1.2	-	-	3.7
OL + ET	1.3	9.1		3.5
Location 2				
OL	2.1	12.2	-	-
SM	2.2	-	10.2	-
ET	2.3	-	-	4.5
OL + SM +ET	2.4	4.1	5.4	4.2

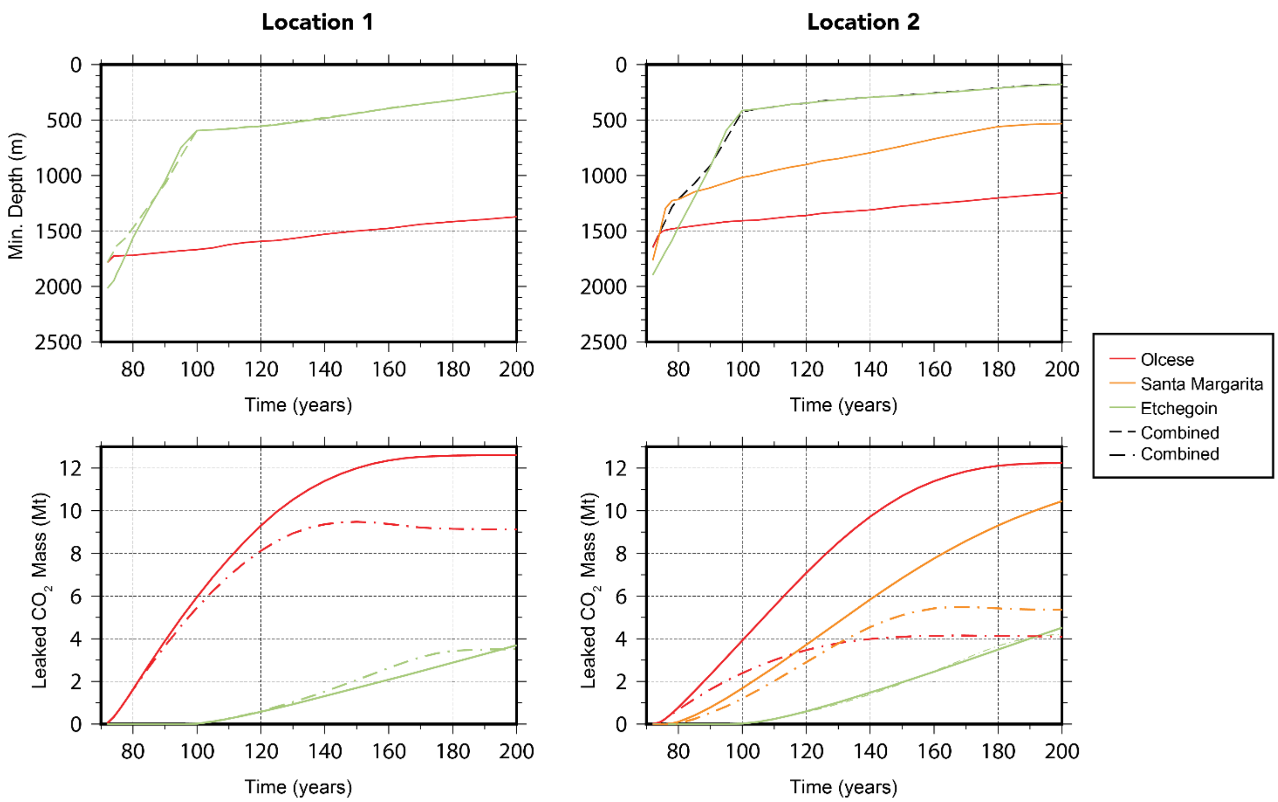

Figure 5. Evolution of leaked CO_2 mass entering thief zones (bottom) and minimum depth reached by the CO_2 (top) as a function of time for each leakage scenario considered in location 1 (left) and location 2 (right). The dash-dot lines are used for the scenarios involving multiple thief zones, red color is for CO_2 reaching the Olcese Fm, Orange the Santa Margarita Fm and green the Etchegoin Fm.

3.4 Simulation results: CO_2 behavior in the subsurface

3.4.1 Baseline – Non-leakage scenario

The non-leakage scenario simulates the development of the CO_2 plume in the reservoir for the expected conditions of operations and post-injection of the hypothetical Kimberlina CCS site. This scenario constitutes the reference case, or baseline, that will be used to evaluate the difference in gravity response corresponding to CO_2 leakage. In this baseline scenario, the sealing Pond-Poso-Creek fault acts as a boundary in the reservoir and leads to a gradual accumulation of CO_2 along this fault. CO_2 reaches the fault about 40 years after the beginning of injection (Figure 6). Because of the updipping stratigraphy of the Vedder Formation and CO_2 buoyancy, CO_2 gradually reaches the shallower parts of the reservoir (approximately 1,500 m deep) laterally along the fault to the southern part of the model domain, with CO_2 saturation ranging from 0.5 to 0.6 (Figure 6). Net density changes within the reservoir are shown in Figure 7 at the end of the injection and at the end of the monitoring period (200 years). The maximum density changes are located at the injection point with values approaching -75 kg/m^3. The net density changes are small in most parts of the reservoir, with values ranging from -20 to -60 kg/m^3 (Figure 7).

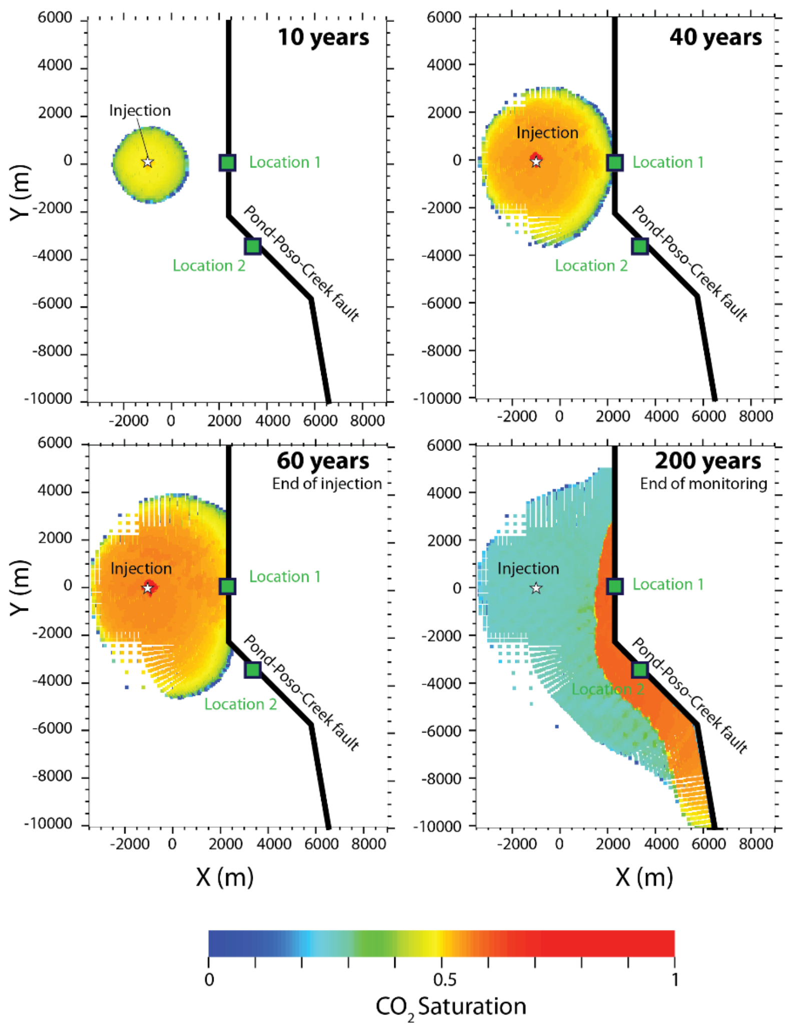

Figure 6. Plan view from above of time-dependent CO_2 saturation within the storage formation (baseline scenario) at 10, 40, 60 and 200 years. CO_2 accumulates along the sealing fault and migrates to the shallower portion of the dipping reservoir. Locations of CO_2 leakage (not active) are indicated for reference.

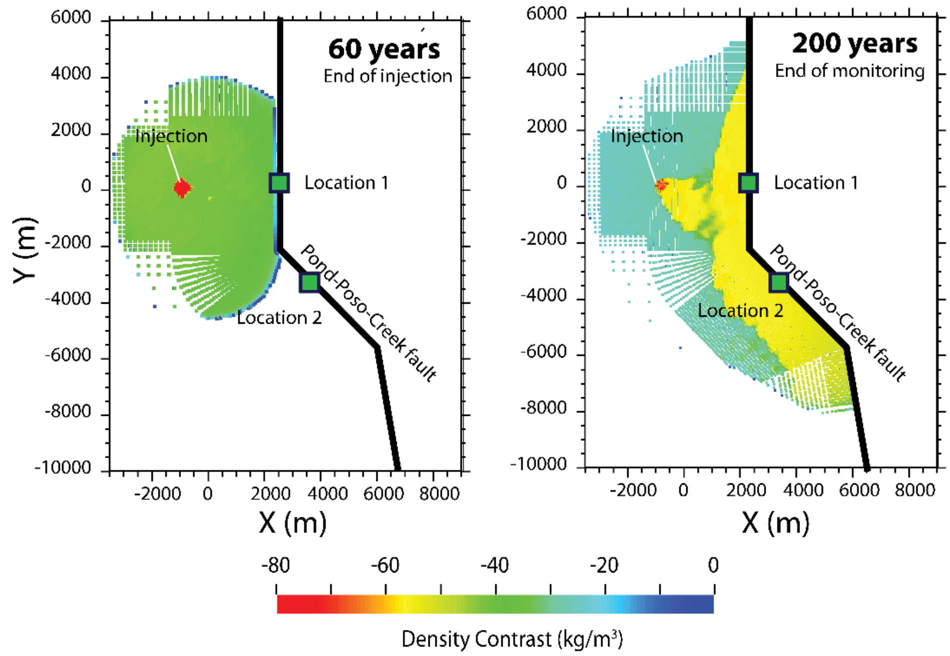

Figure 7. Plan view from above of the net change in density (kg/m^3) at 60 years (end of injection) and 200 years (end of monitoring)

3.4.2 Leakage scenarios at location 1

In the first set of leakage scenarios (location 1, Table 2), CO_2 migrates and accumulates along the fault and toward the shallower parts of the storage formation in a similar way to the baseline scenario. At 70 years, the leaky fault progressively leads to the development of secondary CO_2 plumes in the thief zone(s), either Olcese, Etchegoin or both. CO_2 saturation ranges from 0.3 to 0.5 in the secondary CO_2 plumes, plotted in Figure 8 (top). Although the total leaked CO_2 mass in the Etchegoin formation is smaller (about 2 Mt at 200 years) than that in the Olcese formation (12.36 Mt at 200 years), the largest extent of the plume is observed in the Etchegoin formation. While CO_2 saturation values are relatively comparable in the two thief zones, the net density changes observed are significantly different, reaching a maximum change of about -64 kg/m^3 in the Olcese Formation (Thief zone 1), and -150 kg/m^3 in the Etchegoin Formation (thief zone 3). These differences observed in the two formations are directly associated to the change of CO_2 density properties with depth, illustrated in Figure 1.

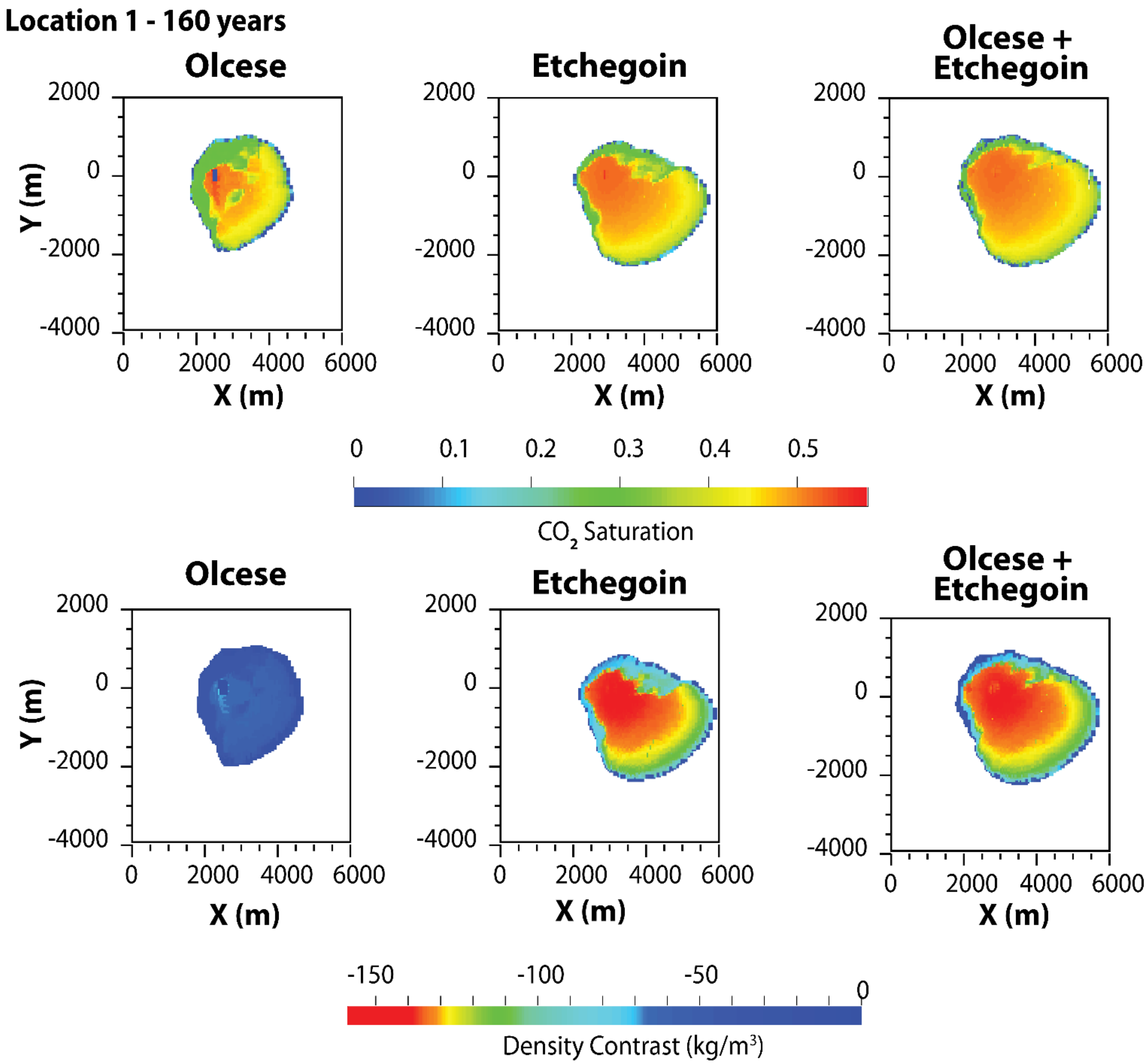

Figure 8. Plan views from above of CO_2 saturation (top) and net density changes in kg/m^3 (bottom) at 160 years for the three leakage scenarios evaluated at location 1. Only the CO_2 saturation and net density changes associated with leakage into the thief zone(s) are plotted.

3.4.3 Leakage scenarios at location 2

For the second set of leakage scenarios (location 2, Table 2), a similar CO_2 behavior is observed in the reservoir, with secondary plumes developing either in the Olcese, Santa Margarita, Etchegoin or in all three thief zones (Figure 9). Similar ranges of CO_2 saturation are observed in all three thief zones, with maximum saturation of 0.6 observed in the vicinity of the injection point. The net density changes are however significantly different, with maximum density changes reaching more than -58 kg/m^3 in the Olcese, -92 kg/m^3 in the Santa Margarita and -158 kg/m^3 in the Etchegoin formations.

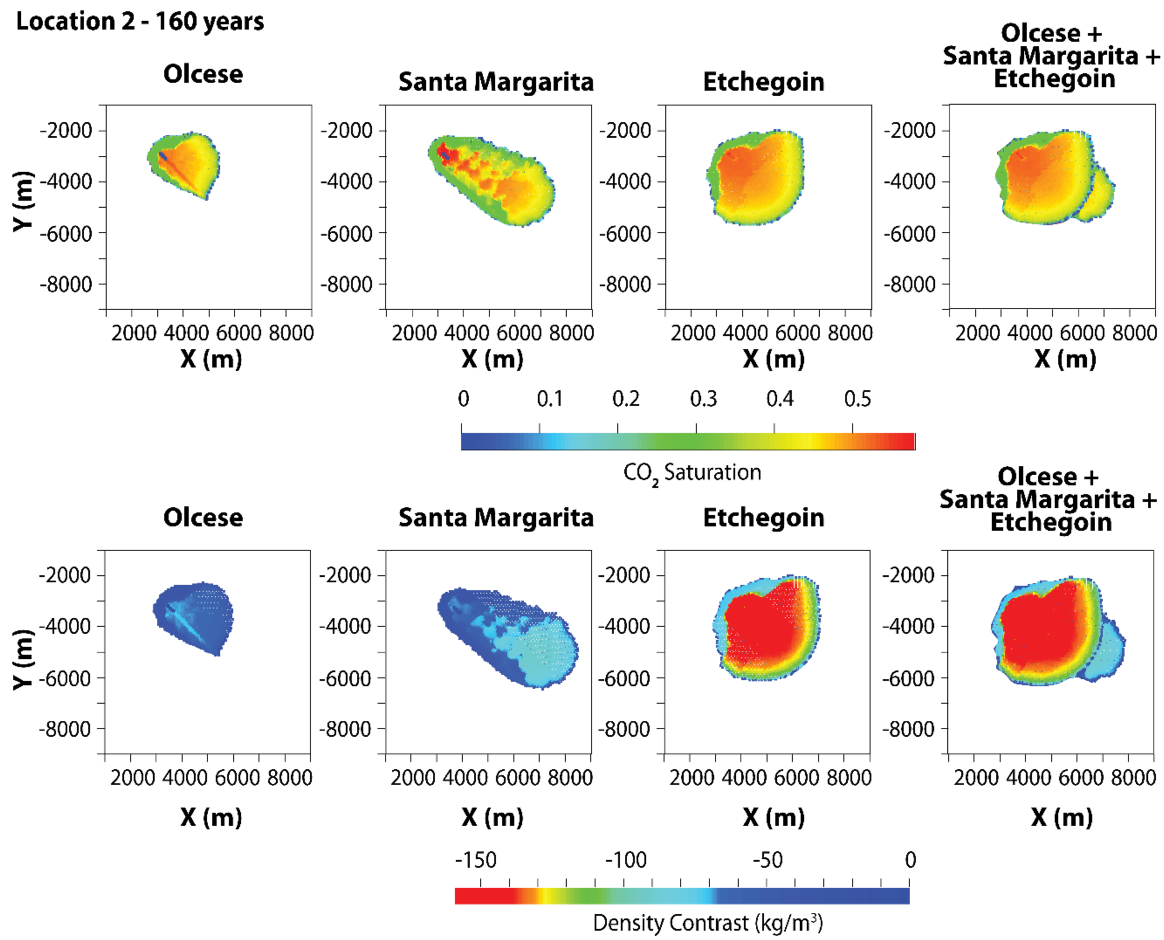

Figure 9. Plan views from above of CO_2 saturation (top) and net density changes in kg/m^3 (bottom) at 160 years for the four leakage scenarios evaluated at location 2. Only the CO_2 saturation and net density changes associated with leakage into the thief zone(s) are plotted

4. Gravity Forward Modeling

GRAV3D v5.0 (UBC-Geophysical Inversion Facility, 2017) was used for carrying out forward modeling of the vertical component of the gravity response (g_z) to a 3D volume of density contrast. g_z is computed using an analytical solution from Haaz (1953), with a calculation based on a collection of rectangular prisms with varying densities.

For each leakage scenario, a density model was built based on the outputs of the TOUGH2-MP Kimberlina 2 model using the parameters of equation 1 (i.e., porosity, CO_2 saturation, brine density and CO_2 density). The model domain was discretized into a 3D orthogonal mesh, with cells of dimensions 50 m × 50 m × 25 m. Each cell was given a density anomaly, or density contrast, corresponding to the density difference between the time step considered and the pre-injection phase (i.e., time = 0 year). A grid of 12,500 × 16,000 m with station spacing of 200 m was used to compute the surface gravity anomaly.

Threshold values of 4, 7 and 10 µGal are chosen to assess the performance of the gravity method to detect CO_2 leaks. These values are in the ranges of repeatability level reported at the CO_2 injection site of Sleipner (Landrø and Zumberge, 2017), or at Prudhoe Bay (Alaska) for monitoring of water flooding operations (Ferguson et al., 2007).

The vertical component of gravity was also calculated in vertical boreholes deployed in the vicinity of the injection point and of the fault in order to assess the performance of the method to detect CO_2 with measurements taken every 20 m.

5. Forward modeling Results

5.1 Using time-lapse gravity for reservoir monitoring: time to detection, frequency of surveys and contribution of borehole measurements

The gravity anomaly associated with the CO_2 migration in the Vedder Formation while the Pond-Poso-Creek fault remains sealed is calculated using the forward modeling steps described above. The CO_2 plume growth, migration in the dipping reservoir and accumulation along the structural feature can be detected from surface measurements as plotted in Figure 10. The magnitude of the gravity anomaly grows to a maximum of -33 μGal reached at 90 years, 20 years after the leak is initiated. This maximal value is found up dip of the injection point for all time steps. The CO_2 plume reaches the Pond-Poso-Creek fault after 40 years of injection and the CO_2 accumulation along the sealed fault becomes detectable in the gravity response at 90 years, with the development of an asymmetrical anomaly, while injection operations are over. Over time, the buoyancy-driven plume migrates into the shallower parts of the reservoir and the associated gravity anomaly magnitude increases. In the baseline scenario, the maximum gravity response occurs at 80 years, with an anomaly of -33 μGal, up dip of the injection point, corresponding to a net change of density of -90 kg/m^3 in the reservoir. Then the signal magnitude decreases due to the spreading of the plume to southeastern and upper part of the reservoir.

The time to detection and frequency of gravity surveys can be obtained from the profile of the evolution of the maximum surface gravity anomaly over time (Figure 11). The time to detection of the CO_2 injected in the reservoir was determined for three threshold values (i.e., 4, 7 and 10 μGal) and is illustrated in Figure 11 and reported in Table 3. Using a threshold of 4 μGal, the gravity anomaly associated with the CO_2 injected in the reservoir can be detected as soon as 6 years after injection starts (15 Mt of CO_2 injected), compared to 10 and 15 years for thresholds of 7 and 10 μGal respectively (25 and 37.5 Mt of CO_2 injected). Additionally, the change of gravity anomaly over time is shown in Figure 11 where a steep gradient of -0.67 μGal/yr occurs during the first 30 years of injection (yellow points and line) and a shallower slope of -0.32 μGal/yr (orange line) occurs during the following 30 years. These gradients show that surface gravity surveys could be conducted every 6, 10 or 15 years for thresholds of 4, 7 and 10 μGal in order to detect the maximum change in the signal during the first 30 years of injection whereas the frequency of surveys could be decreased after 30 years as the evolution of gravity over time is less significant. During the post-injection period, the slope is even smaller (about 0.1 μGal/yr) and the frequency of surveys can be set to a minimum value. However, both monitoring strategy and frequency of surveys should also take into account the tracking of the shape of the plume and not only the detection of the maximum of signal magnitude. Should any divergence from the prediction be detected on the plume shape, the monitoring would need to be pursued at the same or even greater frequency.

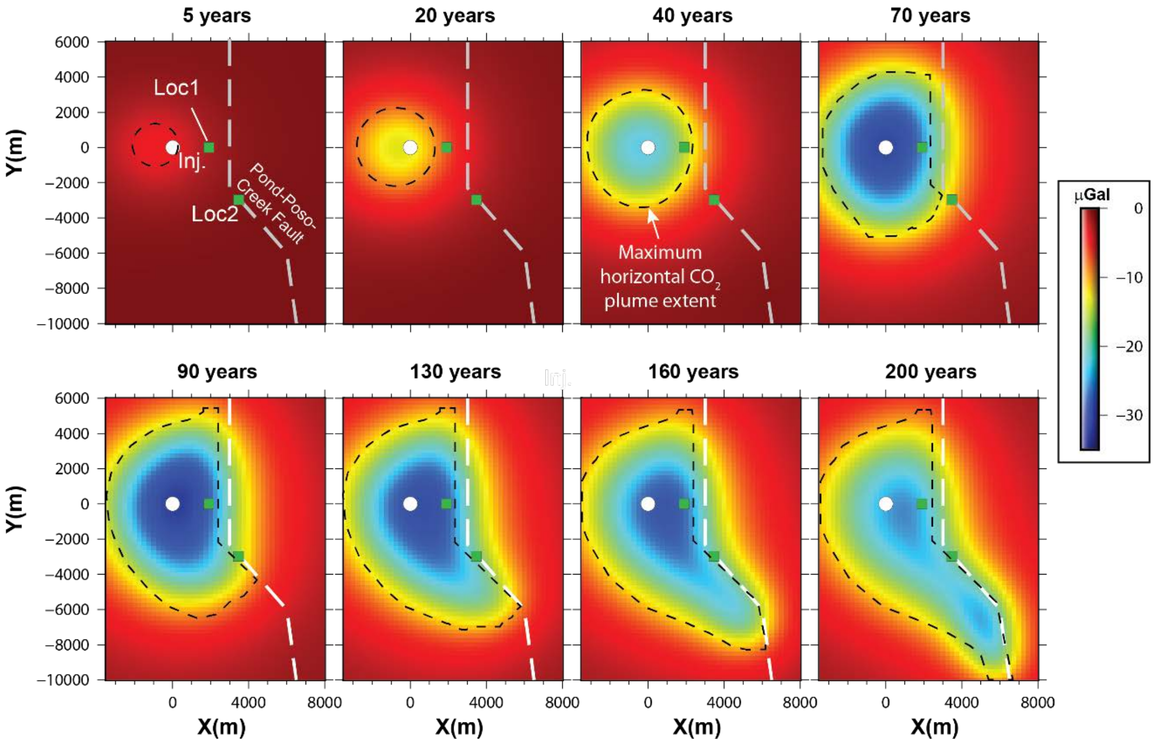

Figure 10. Change in gravity over time for the baseline (no leak) scenario relative to the pre-injection stage. Note the development of an asymmetrical, south east trending, gravity response due 1) to the presence of the sealing fault along which the CO_2 accumulates, and 2) to the geometry of the reservoir itself. Injection point ("Inj."), locations 1 and 2 ("Loc1" and "Loc2") and maximum CO_2 plume extent (black dashed line) are plotted for reference.

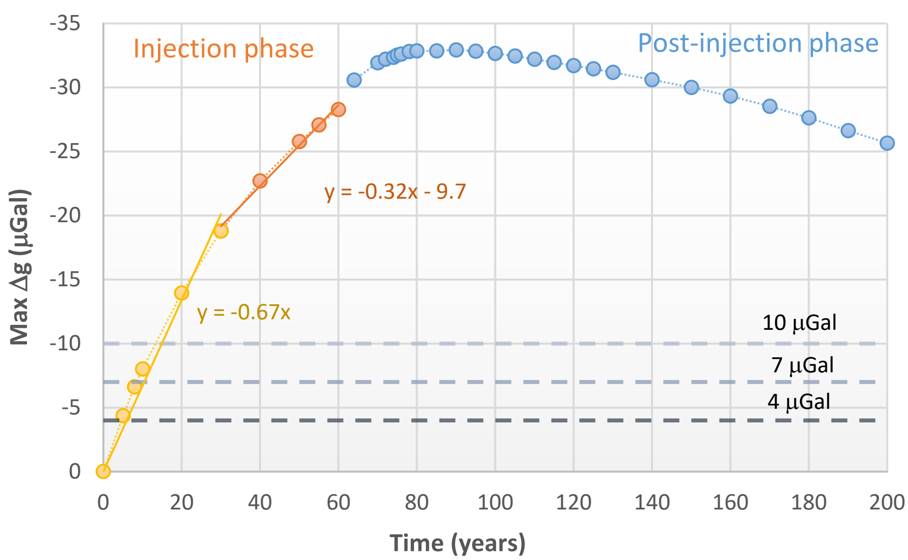

Figure 11. Evolution of the maximum surface gravity anomaly over time for the baseline scenario. The 4, 7 and 10 μGal detection thresholds are also indicated (see text for explanation).

Table 3. Time to detection of the CO_2 injected in the reservoir using surface gravity measurements (no leakage), with threshold values of 4, 7 and 10 μGal

Gravity Threshold (μGal)	**Time to detection** (years)	**Mass of CO_2 injected** (Mt)
4	6	15
7	10	25
10	15	37.5

In addition to surface gravity measurements, time-lapse changes of g_z in boreholes are calculated in three boreholes. For these borehole measurements, a conservative value of 10 μGal can be considered for the detection threshold. The first borehole is located right at the CO_2 injection point while the others are located at locations 1 and 2 (Figure 12). The results show that very soon after the beginning of the injection, a very strong response is observed. For instance, 5 years after the start of injection (12.5 Mt of CO_2 injected), g_z reaches a magnitude of -140 μGal at the injection depth. The gravity anomaly keeps increasing over time and reaches a maximum of -180 μGal at 130 years before decreasing again. At location 1, the gravity anomaly starts being detectable at 70 years with a magnitude of about -50 μGal at the depth of 2300 m and reaches a maximum magnitude of about -130 μGal at 180 years. At location 2, the furthest borehole from the injection well, the gravity signal indicates an anomaly at a depth of 2000 m which does not exceed -25 μGal. The time to detection of the gravity anomaly is directly related to the migration of the CO_2 plume in the reservoir and gives an excellent indication of the depth of the CO_2 in the reservoir. These borehole measurements provide information about the depth and vertical extent of the density anomaly, which could later be used as a constraint in gravity inversions or when modeling surface responses.

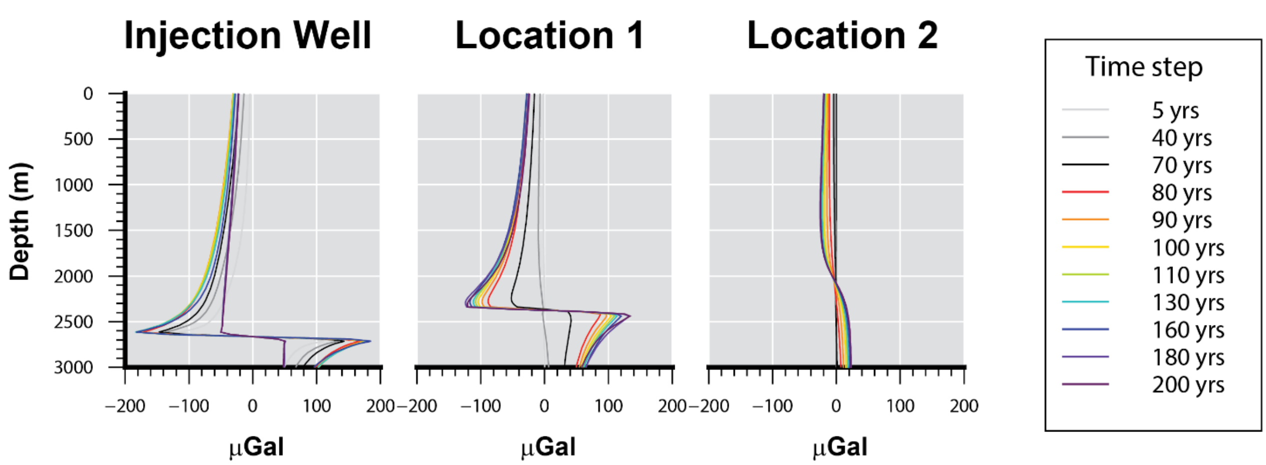

Figure 12. Changes in borehole vertical profile of the vertical component of g (g_z) in the Injection well, and at the Locations 1 and 2, where leakage in not occurring.

5.1 Tracking secondary plumes with time-lapse gravity

The change in the vertical component of gravity for the different leakage scenarios was determined using both surface-based and borehole data. As the leaky windows become active at 70 years, previous time-steps are not considered because they are the same as the baseline scenario.

5.1.1 Surface measurements

In the first leakage scenario (location 1), the leak occurs at a depth ranging from 1300 to 1800 m (Figure 5) and about 12 Mt of CO_2 leaks into the Olcese Formation. The baseline model response is subtracted from the response at each time step in order to determine the signal exclusively associated with the leak and plotted in Figure 13a for four time-steps: 90, 130, 160 and 200 years. The maximum gravity response over time is reported in Figure 14 and the times to detection of the leak corresponding to the three detection thresholds considered (i.e., -4, -7 and -10 μGal) are reported in Table 4. The gravity response associated to the migration of CO_2 into the Olcese Formation reaches the minimum detection threshold of -4 μGal at 90 years, and -10 μGal at 110 years. Over the following decades, the gravity response remains relatively constant and limited, with a maximum value of -15 μGal observed at 160 years (Figure 13a).

Responses associated with the migration of CO_2 into the shallowest thief zone, the Etchegoin formation, and a combined leakage into the Olcese and Etchegoin thief zones are also plotted in Figures 13b,c and Figure 14. While the overall leaked CO_2 mass is considerably lower than for the leak occurring in the Olcese only (4 Mt at 200 years as compared to 12 Mt), the gravity anomaly exclusively associated to the leak becomes detectable as soon as 100 years for a threshold of -4 μGal (Figure 14), which corresponds to the time of arrival of the CO_2 into the Etchegoin formation (Figure 5). The gravity anomaly keeps increasing over time and reaches a magnitude of -170 μGal at 200 years (Figure 13b). In addition to the magnitude of this anomaly, a larger areal extent is observed which is directly related to the larger volume that the CO_2 in a gaseous phase occupies in the porous space at this depth. The asymmetry observed in the gravity anomaly, extending along a northwest-southeast profile is directly related to the regional dip and the subsequent buoyancy-driven migration of CO_2 into the shallower parts of the thief zone.

Figure 13 and Figure 14 also show the results for the combined-leakage scenario, simultaneously into the Olcese and Echtegoin formations. These results support the fact that the contribution of the leak into the Olcese on the overall vertical component of the gravity response is very limited compared to the contribution of the leak occurring in the shallow thief zone. In both cases, the surface vertical component of gravity response demonstrates the presence of a leak.

Table 4. Times to detection of the leakage evaluated for three detectability thresholds and with leakage starting at 70 years

Threshold value (μGal)	Time to detection (years) at location 1			Time to detection (years) at location 2			
	OL	ET	OL+ET	OL	SM	ET	OL+SM+ET
4	90	100	90	90	90	100	90
7	95	110	95	100	100	100	90
10	110	110	100	110	110	100	95

OL=Olcese, ET=Etchegoin, SM=Santa Margarita

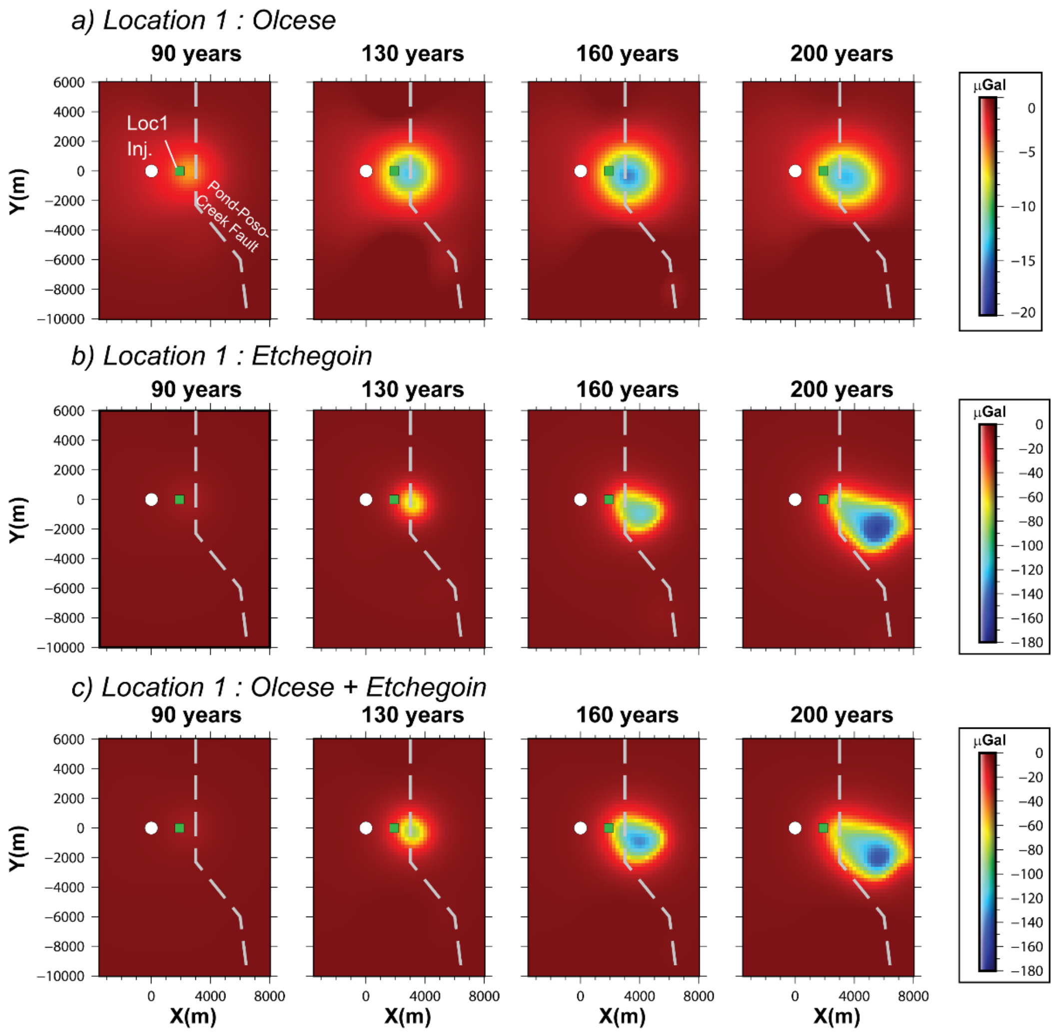

Figure 13. Difference between the surface gravity response associated with a leak occurring into a) the Olcese thief zone ; b) the Etchegoin thief zones, c) the Etchegoin and Olcese thief zones, and that with the baseline scenario for the same time steps (90, 130, 160 and 200 years).

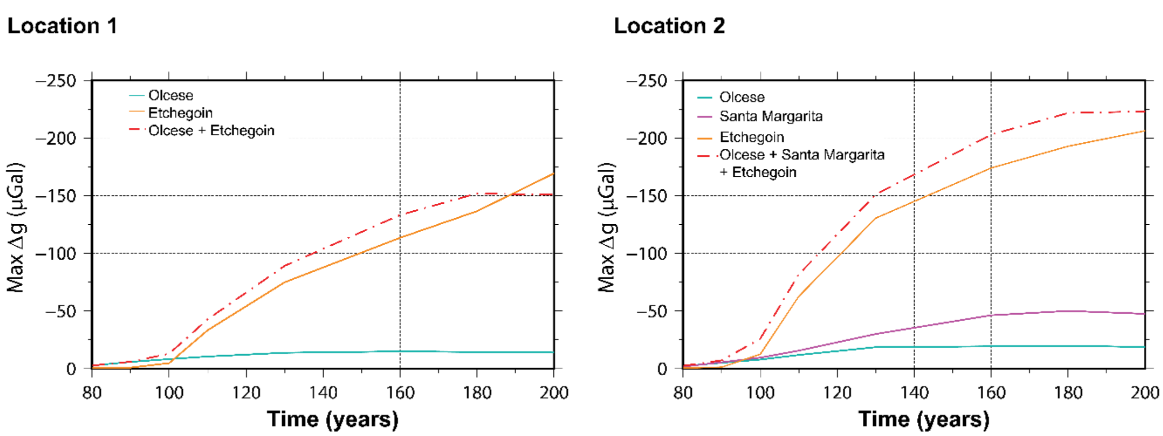

Figure 14. Maximum surface gravity anomaly calculated over time for the different leakage scenarios (left: Location 1 scenarios; right: Location 2 scenarios). The gravity response from the reservoir has been removed.

The same method was used to calculate the surface gravity response for the second set of leakage scenarios (Location 2, Table 2). This leaky window is located ~6 km southeast of the injection well, and the leakage occurs either in the Olcese, Santa Margarita, or Etchegoin formations separately or in all formations at once. The results of maximum surface gravity anomaly and leaked CO_2 mass as a function of time are presented in Figure 14. Maps of the surface gravity anomalies for the four scenarios at four different times are shown in Figure 15 and times to detection are presented in Table 4. The presence of leakage is established for the four scenarios with a maximum gravity response located first up dip of the leaky point, and that gradually migrates to where the CO_2 accumulates in the shallower parts of the reservoir.

The four scenarios evaluated at location 2 present similarities to the first set of leakage scenarios described above. The main difference is the magnitude and the shape of the gravity anomalies. Overall, due to the shallower depths at which the well intersects the thief formations, the magnitude of the gravity anomalies is slightly higher for this set of scenarios. For instance, the gravity response reaches a magnitude of -20 μGal at 200 years for a leak occurring in the Olcese Formation at location 2, as compared to -15 μGal at location1 at the same time and for the same mass of CO_2 leaked (12 Mt). Similarly, the magnitude of the gravity anomaly associated to leak occurring in the Etchegoin formation (Figure 14c), reaches a maximum value of -167 μGal at 200 years at location 1 compared to -204 μGal at location 2. The leak occurring in the Santa Margarita formation only (Figure 14b) leads to a maximum gravity response of -50 μGal observed at 180 years, when 9 Mt of CO_2 leaks out from the reservoir (6% of the total mass injected). An elongation of the anomaly in the southeastern direction is observed. Additionally, in the case of multiple leaks, the presence of CO_2 in the shallowest thief zone is the principal contributor to the surface gravity response.

The times to detection for the four scenarios evaluated at location 2 (Table 3) are overall reduced compared to the first set of scenarios, which is directly related to the geometry of the reservoir, and more specifically to the shallower depths of the three thief zones.

Although gravity surface measurements cannot discriminate alone the existence and depth of multiple CO_2 accumulations in formations located at different depths, additional value of gravity techniques for leak investigation comes from combining the surface-based measurements presented here with borehole-deployed measures that will be presented in the next section.

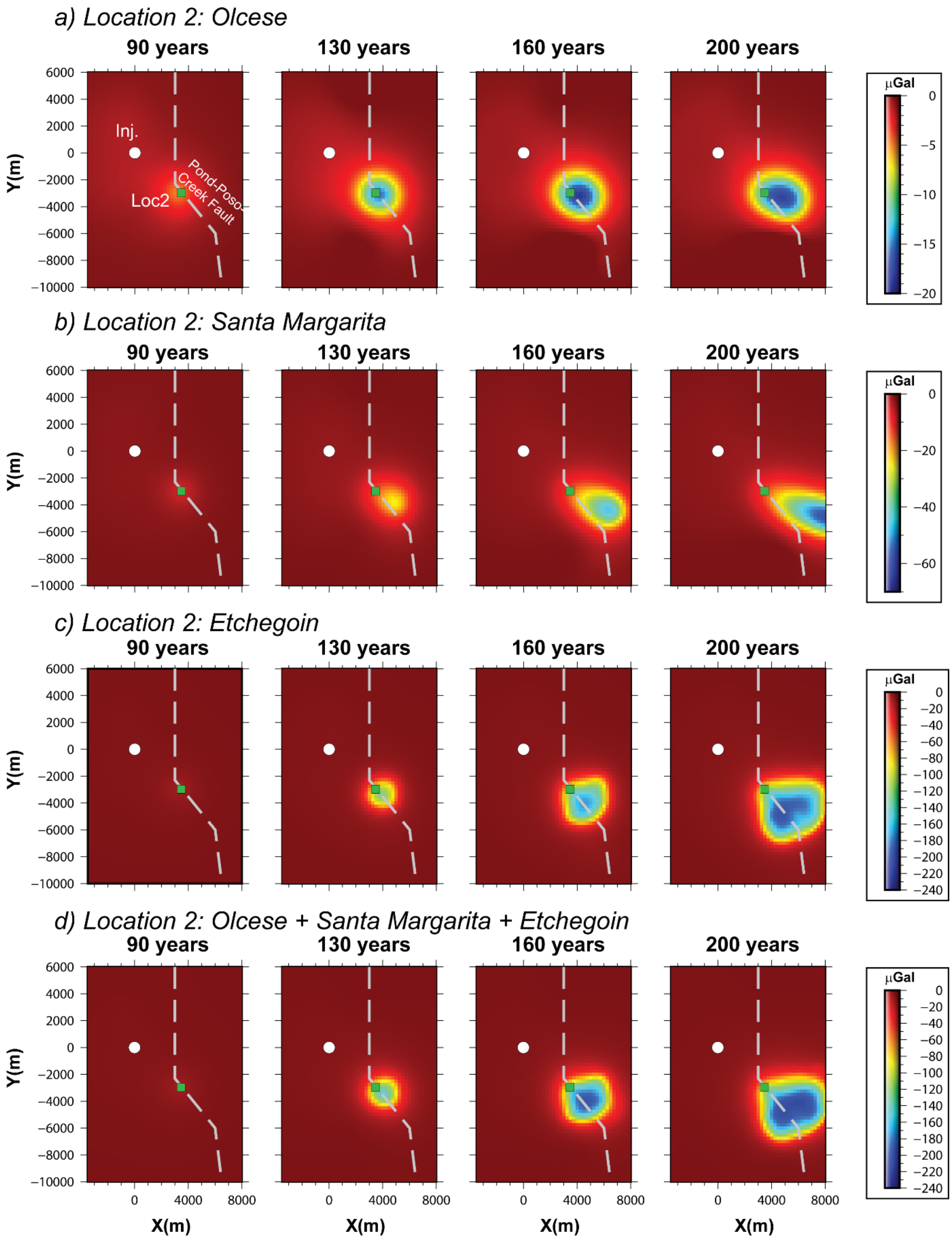

Figure 15. Differences between the surface gravity response associated with a leak into thief zones minus the baseline scenario for the same time steps (90, 130, 160 and 200 years): a) Olcese; b) Santa Margarita); c) Etchegoin; and d) the three thief zones combined.

5.1.2 Borehole measurements

In order to determine if accumulation of CO_2 in multiple formations could be discriminated borehole measurements are considered. The time-lapse changes of g_z are calculated in the three boreholes presented in section 5.1 assuming simultaneous accumulation of CO_2 into the three thief zones at location 2 (scenario 2.4, in Table 2). The results (Figure 16) indicate that the depths of the three thief zones can clearly be distinguished using this method in the wells that intersect the density anomalies. The leak occurring in the shallowest formation (Etchegoin formation, about 500 m deep) yields a significant gravity response with values ranging from -100 to -300 μGal, depending on the time considered. The sensitivity of the borehole gravity method with the distance from the edge of the CO_2 plume is not modeled for this scenario, but as demonstrated by Gasperikova and Hoversten (2008), the responses decrease away from the edge of the density anomaly. Several tests (not represented here) have been performed with wells located at increased distances of Location 2 and no borehole-gravity response is observed beyond a distance of 250 m. Overall, it is clear that depths and extent of the density anomalies associated with multiple thief zones can be captured using borehole gravity measurements provided they are not too far away for the leakage paths.

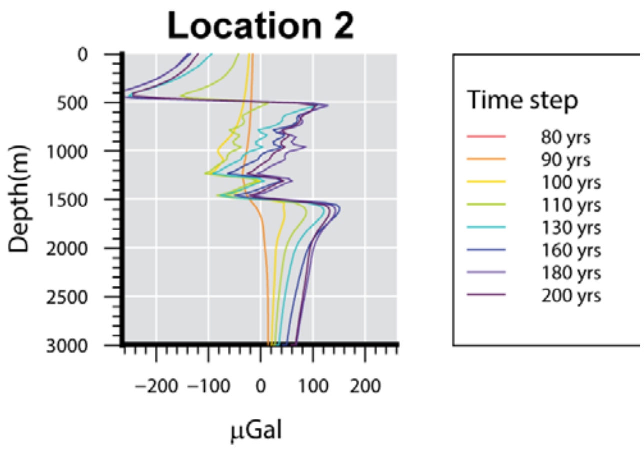

Figure 16. Changes in vertical component of g (gz) in a borehole at Location 1 where leakage is occurring (scenario 2.4, Table 2).

6. Inversion: estimating the mass of leakage

The usefulness and sensitivity of the time-lapse gravity method based on forward modeling of density anomalies deduced from a multi-phase flow model of the growth and migration of a CO_2 plume has been demonstrated. It is now opportune to test some inverse modeling approaches in order to evaluate the potential of these methods to detect and estimate the change in fluids density in the porous space as given by equation 1 and thus estimate the mass of leaked CO_2. The gravity anomaly calculated by forward modeling for one scenario and at a specific time step is used and called “observations data” for the simplicity of the discussion. The scenario 1.3 (Table 2) has been selected at 160 years, 100 years after the end of the injection. This set of pseudo “observations data” at 160 years, with a standard deviation of 2% added to each data, will be inverted with two objectives: 1) getting a reasonable idea of the initial density distribution used to generate the gravity anomaly and 2) testing the best set of parameters to be used in this inversion. In other words, can gravity inversion of time-lapse survey data be able to detect a leakage, determine its location and shape and estimate its corresponding mass?

For this approach, the UBC-GIF GRAV3D inversion software is used. The inverse problem is formulated as an optimization problem where a global objective function is minimized. This global objective function has two components: a data misfit function which is responsible for ensuring the model predicts data that fits the field observations and a model objective function which ensures that the model contains plausible geological structures (UBC-GIF, 2017). In the present case, the model objective function is changed by prescribing the range of minimum and maximum values for the density anomalies and by prescribing or not a density distribution as initial and reference models. This reference density distribution is coming from the modeled baseline scenario at a specific time-step in order to mimic the reality where the operator would only have as a reference the baseline simulation updated by observations. The baseline density distribution at 70 years (i.e., 10 years after the end of injection), corresponding to the beginning of leakage, was chosen as the reference.

The set of observations incorporate both surface and borehole observations. Several cases have been studied: inversion of surface observations alone with or without a reference model and then joint inversion of surface and borehole observations. These cases are summarized in Table 5, column 1. It should be noted that no inversion of surface observations alone is presented because it results to unrealistic concentration of all the CO_2 close to the surface.

Table 5. Equivalent mass of displaced fluids (brine and CO_2) in Mt for different inversion cases above two depths and for the whole domain. The 500 m depth corresponds to the base of the Etchegoin formation and the 1600 m depth relates to the minimum depth reached by the main plume in the reservoir. Any mass detected above this depth must be considered as anomalous and resulting from a leakage. The masses of CO_2 used in the multiphase flow simulation of the corresponding leakage scenario are provided on line 1 for comparison.

	Mass of displaced fluids (Mt) for		
Inversion Cases	depth < 500 m	depth < 1600 m	whole domain
Reference forward model at 160 years (*Figure 17,* leakage at location 1 into Olcese and Etchegoin formations), the inversion results are compared to these values. The corresponding CO_2 masses used for the leakage scenario simulation are in red.	**9.5** (*2.6*)	**32.4** (*12.2*)	**119.5** (*122.2*)
1) Only surface data – with 70 years baseline scenario as reference *(Figure 18)*	1.9	14.7	123.4
2) Surface data + a dense network of boreholes without reference *(not represented)*	11.7	35.8	115.0
3) Surface data + four boreholes over the leakage zone			
3a) with no reference file *(not represented)*	9.4	51.5	110.8
3b) with 70 years baseline scenario as reference *(Figure 19)*	8.7	39.2	115.9

The fluid density distribution at 160 years to which the results of the inversion should be compared is shown in Figure 17.

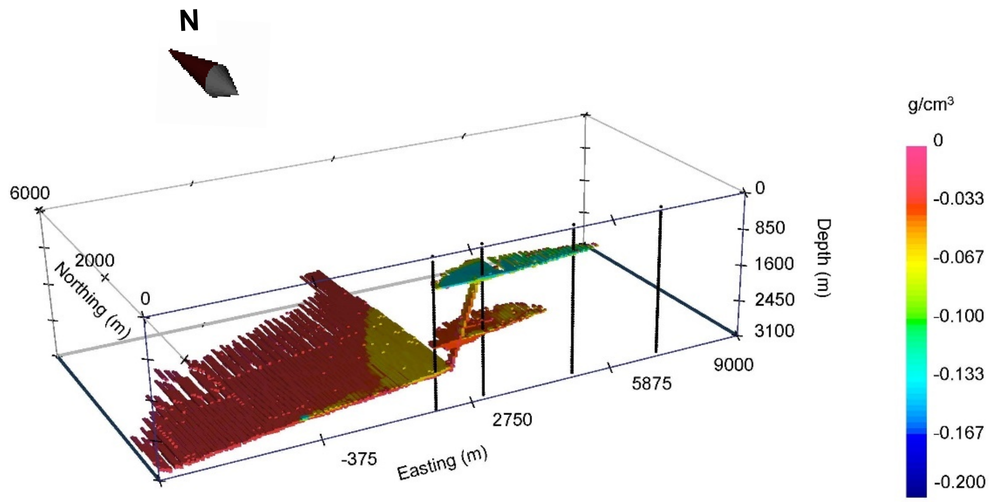

Figure 17. Half-plume (cut at y=-50m) for the reference scenario at location 1 at 160 years. The corresponding surface gravity anomaly will be used used for the inversion. The color scale gives the density anomaly compared to baseline scenario at 0 years. The four vertical black lines correspond to the virtual boreholes used in the inversion.

Inversion results for two cases are illustrated and discussed. For the first case (case 1, Table 5), one can observe (Figure 18) that the overall shapes of the plume in the reservoir as well as the region interested by the leakage are in good accordance with the initial model but that the estimated masses for the depths above 1600 m don't match the ones used in the reference case.

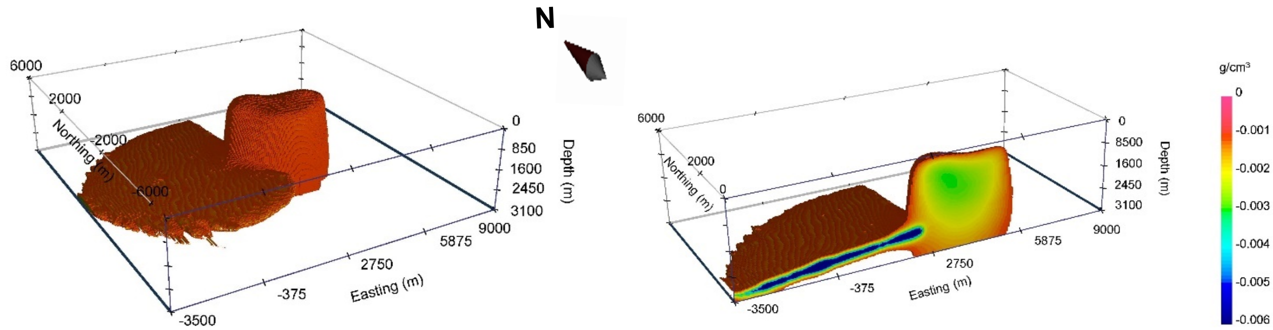

Figure 18. Density anomaly distribution resulting from the inversion of surface observations only and using 70 years baseline reference model (case 1, Table 5). Left: full plume; right: cross section at y = -50 m.

For the second case (case 3b, Table 5), surface observations are jointly inverted with observations from four boreholes located along a profile crossing the leaked plume using the baseline at 70 years as a reference model. Figure 19 shows a good correspondence of the overall shape of the plume in the main reservoir and a very good definition of the CO_2 plume in both thief zones. The values of the estimated masses (case 3b, Table 5) are in good agreement with the ones obtained in the reference case. The other cases are not represented but one should note that cases 2 and 3a (Table 5) also give satisfactory results.

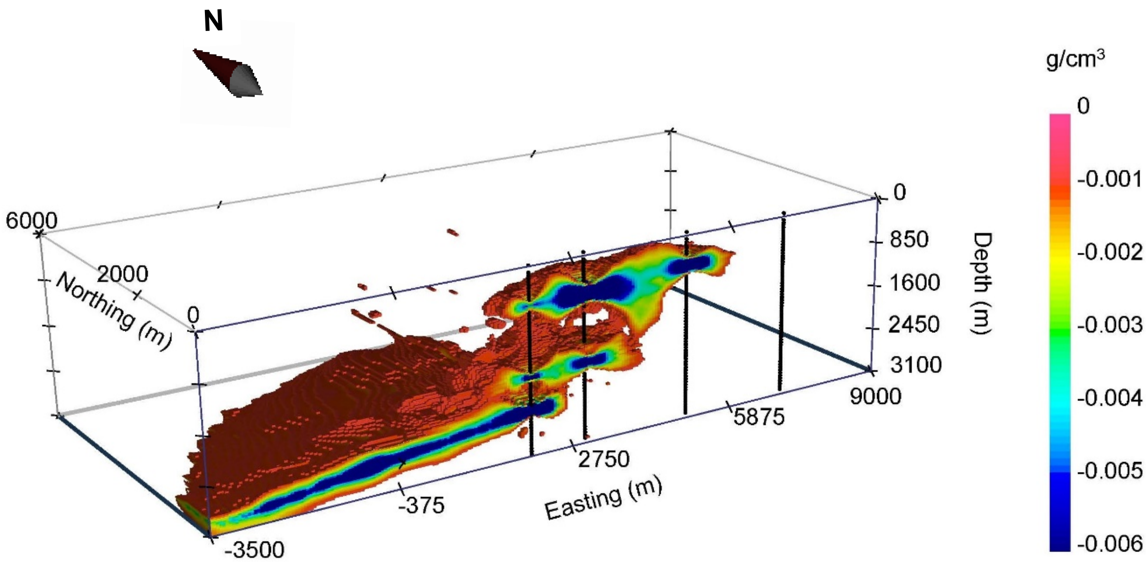

Figure 19. Cross section at y=-50 m of the density anomaly distribution resulting from the inversion of surface and four borehole observation without a reference file (case 3b, Table 5). The boreholes are represented as vertical black lines.

Inversion of gravity observations gives the best results when borehole data and surface data are jointly used with the baseline density distribution at 70 years as a reference to constrain the model objective function.

7. Discussion

7.1 Approaching the detection threshold of a CCS site with an analytical solution

The results of the multiphase flow simulations show that once a leak occurs, CO_2 migrates upward and accumulates in overlying permeable thief zones. The buoyancy-driven CO_2 accumulates at the top of the thief zones and the CO_2 plume grows laterally forming elongated or circular shapes with associated thicknesses ranging from 20 to 30 m. Figure 20 shows the minimum leaked CO_2 mass leading to a gravity anomaly greater than 10, 7 and 4 μGal at the surface as a function of the depth of the leak which is defined as the minimum depth reached by CO_2 during its migration toward the surface. Only the scenarios with a leak to a single thief zone were considered here.

These results were then compared to those provided by a simplified approach which assumes that CO_2 leaks are comparable to vertical cylinders of length ranging from 20 to 30 m (corresponding roughly to the thicknesses of the CO_2 layer accumulation in thief zones), with homogenously distributed density contrast determined based on the conditions found at Kimberlina for a given depth (e.g., brine and CO_2 densities), for a porosity of 25% and a saturation of 30%. Different values of the cylinder masses are then obtained by varying the radius and thus the volume. To calculate the gravity effect of these vertical cylinders, the analytical solution proposed by Telford (1976) is used and the minimum mass capable of producing an anomaly of 10, 7 and 4 μGal is determined (orange, yellow and green lines in Figure 20). The results of this simplified approach agree very well with the surface gravity responses computed from the Kimberlina. This simplified approach can thus be used to give a rough estimate of the detection thresholds that could be expected for any given storage site with specific conditions of temperature, pressure and salinity gradient.

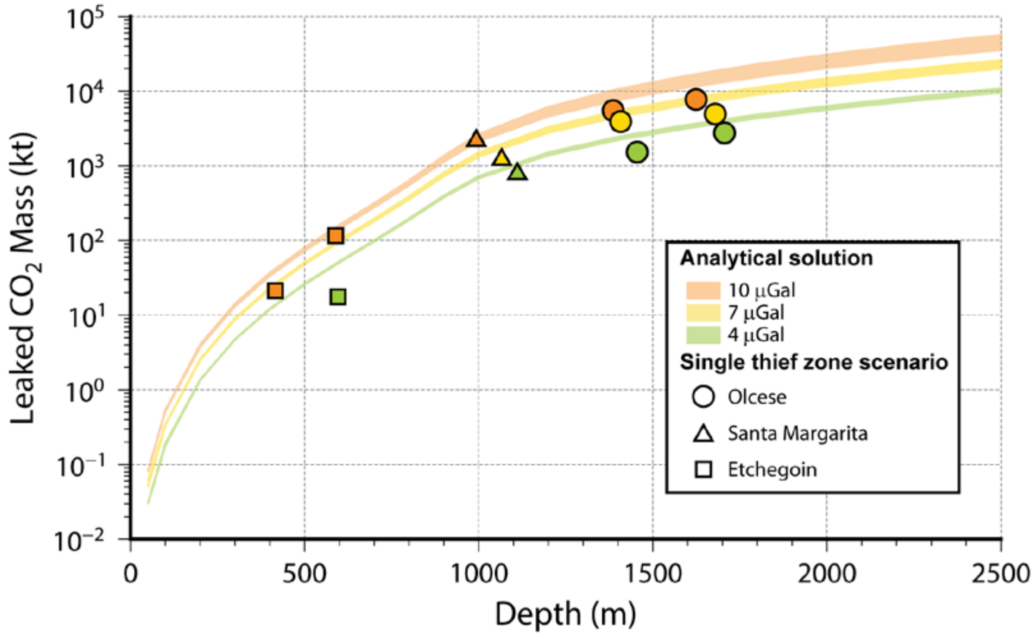

Figure 20. Estimation of the minimum detectable CO_2 mass (in 10^{-3}Mt) capable to create a gravity anomaly of 10 (orange), 7 (yellow) and 4μGal (green) at the surface as a function of depth. Circles, triangles and square symbols correspond to the Kimberlina 2 numerical simulations and color lines correspond to the simplified cylinder analytical solution (Telford, 1976), their thickness correspond to the difference between solutions for the two lengths of the reservoir (20 and 30m).

7.2 Strategy to implement a monitoring network

The spatial extension of the gravity anomaly at the surface depends on the depth, the volume and the magnitude of the density anomaly. When planning the station spacing, consideration should be given to the expected anomaly pattern. Designing an appropriate monitoring network would first consist of considering the maximum extent of the main plume obtained by the multiphase flow modeling and also the minimum size of the anomaly of interest that will determine the minimum spatial sampling rate. For Kimberlina, the maximum extent of the anomaly corresponds to the large 12 × 16 km area shown in Figure 10. In order to cover this area with an appropriate resolution, a baseline survey consisting of a grid with station spacing of 500 m would constitute a reasonable baseline survey before any injection (~800 stations), as illustrated in Figure 21. Such a grid would indeed capture the main pattern.

Regarding the time between two consecutive surveys, results presented in Figure 11 demonstrated that a survey every 6 to 15 years, depending on the detection threshold considered at the site would capture the gravity changes associated to the CO_2 injection. Any deviation from the CO_2 plume baseline scenario for a given time should trigger a redefinition of both the spatial and temporal sampling rates. It is therefore critical to get a high-resolution gravity baseline.

These surveys are relatively inexpensive and easy to deploy and could help deciding when and where more expensive seismic surveys should be performed in the case of observed gravity anomalies going above a pre-defined threshold.

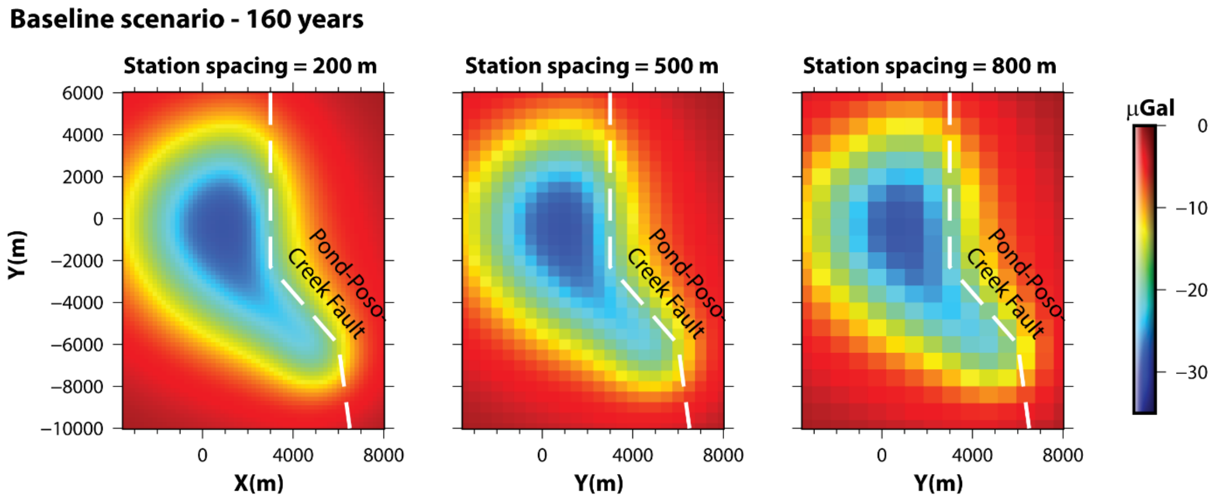

Figure 21. Illustration of the importance of the surface station spacing when defining the monitoring network (from left to right, station spacing is respectively 200 m, 500 m and 800m).

It was demonstrated that borehole measurements of g_z provide excellent constrains in depth only when they are located close (250 m in this study) to the density anomaly associated with the presence of CO_2. Because the gravity response decreases away from the CO_2 plume, the lateral resolution of the measurements is very limited, and borehole gravity measurements should only be considered for leakage detection when the presence of CO_2 is demonstrated or strongly suspected, and the mass of CO_2 needs to be quantified and the depth of the leak be determined with accuracy. Recent progress in three-axis microgravity technology could permit the deployment of such instrumentation into boreholes to measure the two horizontal components of g sensitive to density anomalies far beyond the borehole (Lofts et al., 2019).

Multi-physics models are critical for integrating the geological complexity of a storage site and implementing a risk-based monitoring strategy. When planning the gravity station spacing, consideration should be given to the extent of the predicted anomaly associated to the migration of the CO_2 plume in the reservoir.

At a large and complex site such as Kimberlina, the presence of the fault is known and should be fully integrated in the risk profile of the site. The models considered in this study were not built to represent the real behavior of a fault but provided means of having CO_2 plumes at certain locations and of demonstrating the sensitivity of the method to various CO_2 plume configurations. In these models, it was observed that although the fault starts being conductive 10 years after the end of the injection, it may require few more decades, depending on the detection threshold considered, before any leak can be detected with surface measurements if the CO_2 is migrating toward shallow formations. Conversely, when CO_2 reaches the shallowest formation, even a small to moderate mass of CO_2 triggers an immediate gravity signal that can be measured. While leaks can be detected with surface measurements, their spatial extent may be limited compared to the gravity response associated with the CO_2 plume migration in the reservoir. Additionally, should a large leak occur in a deep formation, it is very unlikely that the gravity method could be used as an early detection method.

These observations are all fundamental when designing a monitoring strategy, but also when discussing the duration of post-injection site care (PISC) periods on CCS sites. Although the leakage scenarios presented in the present study are all theoretical and extreme and meant to assess the sensitivity of geophysical methods, they highlight the importance of making risk-informed decisions when designing and optimizing the monitoring network. They also illustrate clearly the need for careful simulations to identify the most pertinent monitoring tools to be used in early detection of CO_2 leakage.

8. Conclusions

The performance of both surface and borehole time-lapse gravity monitoring to detect CO_2 leakage from the hypothetical Kimberlina storage site, San Joaquin Valley, California, has been evaluated. Two unique sets of leakage scenarios were developed and tested for one storage formation and up to three thief zones using multi-physics-based simulations that were based on the complex geologic model of the Kimberlina site including a steeply dipping fault. The following main conclusions can be drawn:

- Surface-based gravity monitoring of a CCS site during and after injection provide valuable information on the location, shape and volume/mass of the CO_2 plume in the reservoir and can be considered as a valid reservoir management tool. In particular this can help with updating the predictive scenarios by real time comparison of predicted values with observations.
- The surface-based gravity responses obtained for the different leakage scenarios demonstrate that leakage can be detected at the surface in all the scenarios with the masses of leaked CO_2 considered here but the time to detection is highly variable and dependent on the detection threshold considered, location of the leak, and amount of fluid leaked. The magnitude of the gravity signal strongly depends on the depth of the leak(s). The areal extent of the anomaly is extremely well correlated to the CO_2 saturation/density changes occurring in the subsurface allowing a precise mapping of the plume front. However, gravity surface measurements cannot alone discriminate the existence and depth of multiple distinct leaks. These observations are keys to define the monitoring strategy deployed at CCS sites and demonstrate how monitoring needs to be adapted throughout the lifetime of a CCS project.
- The predicted surface gravity changes are small when the source anomaly is located at a depth greater than 1,500 m and a leak occurring at these depths would only be detected if the mass is significant, ranging from about 3 Mt for a detection threshold of 4 μGal to about 8 Mt for a detection threshold of 10 μGal at the hypothetical Kimberlina site, which represent 2 to 5% of the total mass of CO_2 injected.
- Borehole measurements of g_z provide excellent constraints on the mass and depth when they are located in proximity of the density anomaly associated with the presence of CO_2, thus discriminating multiple leaks in different thief zones. However, the deployment of instrumented boreholes in a storage site should be considered cautiously, first because of the intrinsic costs of deep boreholes, even slim holes, and second because of the risk of creating additional leakage pathways for CO_2 by drilling through the containment formations.
- The gravity response expected at the surface for a leak occurring in a single thief zone can be assumed to be equivalent to the vertical gravitational effect of a vertical cylinder
- Inversion of surface data alone can bring valuable information on the occurrence of leakages and their spatial extent providing a reference model based on the density distribution at the end of the injection is used. The best estimate of the mass of leaked CO_2 can only be obtained if boreholes data are jointly inverted.

Multiphase flow simulations followed by gravity modeling are fundamental in order to define if and when gravity monitoring would be applicable at storage sites. This initial step will help design the spatial and temporal sampling strategy for the gravity surveys.

Acknowledgments

The research presented in this manuscript was completed as part of the National Risk Assessment Partnership (NRAP). Funding for this project was provided to Pacific Northwest National Laboratory (PNNL) under DOE contract number DE-AC05-76RL01830 and to Lawrence Berkeley National Laboratory under DOE contract number DE-AC02-05CH11231. The authors wish to thank Thomas

Jacob and an anonymous reviewer for their careful comments that greatly contribute to improve this paper.

9. References

Alnes, H., Eiken, O., Nooner, S., Sasagawa, G., Stenvold, T., Zumberge, M., 2011. Results from Sleipner gravity monitoring: Updated density and temperature distribution of the CO_2 plume. Energy Procedia 4, 5504-5511.

Anderson, S.T., 2017. Risk, Liability, and Economic Issues with Long-Term CO_2 Storage—A Review. Natural Resources Research 26, 89-112.

Bielicki, J.M., Pollak, M.F., Deng, H., Wilson, E.J., Fitts, J.P., Peters, C.A., 2016. The Leakage Risk Monetization Model for Geologic CO_2 Storage. Environmental Science & Technology 50, 4923-4931.

Bielicki, J.M., Pollak, M.F., Fitts, J.P., Peters, C.A., Wilson, E.J., 2014. Causes and financial consequences of geologic CO_2 storage reservoir leakage and interference with other subsurface resources. International Journal of Greenhouse Gas Control 20, 272-284.

Birkholzer, J.T., Zhou, Q., Tsang, C.-F., 2009. Large-scale impact of CO_2 storage in deep saline aquifers: A sensitivity study on pressure response in stratified systems. International Journal of Greenhouse Gas Control 3, 181-194.

Chabora, E.R., Benson, S.M., 2009. Brine Displacement and Leakage Detection Using Pressure Measurements in Aquifers Overlying CO_2 Storage Reservoirs. Energy Procedia 1, 2405-2412.

Chadwick, R.A., Arts, R., Bentham, M., Eiken, O., Holloway, S., Kirby, G.A., Pearce, J.M., Williamson, J.P., Zweigel, P., 2009. Review of monitoring issues and technologies associated with the long-term underground storage of carbon dioxide. Geological Society, London, Special Publications 313, 257-275.

Davis, K., Li, Y., Batzle, M., 2008. Time-lapse gravity monitoring: A systematic 4D approach with application to aquifer storage and recovery. GEOPHYSICS 73, WA61-WA69.

Deng, H., Bielicki, J.M., Oppenheimer, M., Fitts, J.P., Peters, C.A., 2017. Leakage risks of geologic CO_2 storage and the impacts on the global energy system and climate change mitigation. Climatic Change 144, 151-163.

European Union CCS Directive 2009/31/EC of the European Parliament and of the Council of 23 April 2009 on the geological storage of carbon dioxide and amending Council Directive 85/337/EEC, European Parliament and Council Directives 2000/60/EC, 2001/80/EC, 2004/35/EC, 2006/12/EC, 2008/1/EC and Regulation (EC) No 1013/2006 (1). Official Journal of the European Union 2009; L140:114-35.

Dodds, K., R. Krahenbuhl, A. Reitz, Y. Li and S. Hovorka, 2013. Evaluating time-lapse borehole gravity for CO_2 plume detection at SECARB Cranfield. International Journal of Greenhouse Gas Control 18(0): 421-429.

Eiken, O., Stenvold, T., Zumberge, M., Alnes, H., Sasagawa, G., 2008. Gravimetric monitoring of gas production from the Troll field. Geophysics 73, WA149-WA154.

Fabriol, H., Bitri, A., Bourgeois, B., Delatre, M., Girard, J.F., Pajot, G., Rohmer, J., 2011. Geophysical methods for CO_2 plume imaging: Comparison of performances. Energy Procedia 4, 3604-3611.

Feitz, A.J., Leamon, G., Jenkins, C., Jones, D.G., Moreira, A., Bressan, L., Melo, C., Dobeck, L.M., Repasky, K., Spangler, L.H., 2014. Looking for leakage or monitoring for public assurance? Energy Procedia 63, 3881-3890.

Ferguson, J.F., Chen, T., Brady, J., Aiken, C.L.V., Seibert, J., 2007. The 4D microgravity method for waterflood surveillance II --- Gravity measurements for the Prudhoe Bay reservoir, Alaska. Geophysics 72, I33-I43.

Furre, A.-K., Eiken, O., Alnes, H., Vevatne, J.N., Kiær, A.F., 2017. 20 Years of Monitoring CO_2-injection at Sleipner. Energy Procedia 114, 3916-3926.

Gasperikova, E., Hoversten, G.M., 2008. Gravity monitoring of CO_2 movement during sequestration: Model studies. Geophysics 73, WA105-WA112.

Haaz, Z.B., 1953. Relations between the potential of the attraction of the mass continued in a finite rectangular prism and its first and second derivatives (in Hungarian). Geofiz. Kozlemenyek II, 57-66.

Hannis, S., Chadwick, A., Connelly, D., Blackford, J., Leighton, T., Jones, D., White, J., White, P., Wright, I., Widdicomb, S., Craig, J., Dixon, T., 2017. Review of Offshore CO_2 Storage Monitoring: Operational and Research Experiences of Meeting Regulatory and Technical Requirements. Energy Procedia 114, 5967-5980.

Harbert, W., Daley, T.M., Bromhal, G., Sullivan, C., Huang, L., 2016. Progress in monitoring strategies for risk reduction in geologic CO_2 storage. International Journal of Greenhouse Gas Control 51, 260-275.

Hare, J.L., Ferguson, J.F., Aiken, C.L.V., Brady, J.L., 1999. The 4-D microgravity method for waterflood surveillance: A model study for the Prudhoe Bay reservoir, Alaska. GEOPHYSICS 64, 78-87.

Hepple, R.P., Benson, S.M., 2005. Geologic storage of carbon dioxide as a climate change mitigation strategy: performance requirements and the implications of surface seepage. Environmental Geology 47, 576-585.

Herzog, H.J., 2011. Scaling up carbon dioxide capture and storage: From megatons to gigatons. Energy Economics 33, 597-604.

IPCC, 2005. Special report on carbon dioxide capture and storage. Cambridge University Press, Cambridge, UK/New York, NY, USA.

Jacob, T., Rohmer, J., Manceau, J.-C., 2016. Using surface and borehole time-lapse gravity to monitor CO_2 in saline aquifers: a numerical feasibility study. Greenhouse Gases: Science and Technology 6, 34-54.

Jordan, A.B., Stauffer, P.H., Harp, D., Carey, J.W., Pawar, R.J., 2015. A response surface model to predict CO_2 and brine leakage along cemented wellbores. International Journal of Greenhouse Gas Control 33, 27-39.

Jung, Y., Zhou, Q., Birkholzer, J.T., 2013. Early detection of brine and CO_2 leakage through abandoned wells using pressure and surface-deformation monitoring data: Concept and demonstration. Advances in Water Resources 62, 555-569.

Jung, Y., Zhou, Q., Birkholzer, J.T., 2015. On the detection of leakage pathways in geological CO2 storage systems using pressure monitoring data: Impact of model parameter uncertainties. Advances in Water Resources 84, 112–124.

Kabirzadeh, H., Sideris, M.G., Shin, Y.J., Kim, J.W., 2017. Gravimetric Monitoring of Confined and Unconfined Geological CO_2 Reservoirs. Energy Procedia 114, 3961-3968.

Keating, E.H., Fessenden, J., Kanjorski, N., Koning, D.J., Pawar, R., 2010. The impact of CO_2 on shallow groundwater chemistry: observations at a natural analog site and implications for carbon sequestration. Environmental Earth Sciences 60, 521-536.

Keating, E.H., Hakala, J.A., Viswanathan, H., Carey, J.W., Pawar, R., Guthrie, G.D., Fessenden-Rahn, J., 2013. CO_2 leakage impacts on shallow groundwater: Field-scale reactive-transport simulations informed by observations at a natural analog site. Appl Geochem 30, 136-147.

Kim, C.Y., Han, W.S., Park, E., Jeong, J., Xu, T., 2018. CO_2 Leakage-Induced Contamination in Shallow Potable Aquifer and Associated Health Risk Assessment. Geofluids 2018, 19.

Krahenbuhl, R.A., Li, Y., Davis, T., 2011. Understanding the applications and limitations of time-lapse gravity for reservoir monitoring. The Leading Edge 30, 1060-1068.

Krahenbuhl, R.A., Li, Y., 2012. Time-lapse gravity: A numerical demonstration using robust inversion and joint interpretation of 4D surface and borehole data. GEOPHYSICS 77, G33-G43.

Landrø, M., Zumberge, M., 2017. Estimating saturation and density changes caused by CO_2 injection at Sleipner — Using time-lapse seismic amplitude-variation-with-offset and time-lapse gravity. Interpretation, 5(2), T243-T257.

Lawter, A., Qafoku, N.P., Wang, G., Shao, H., Brown, C.F., 2016. Evaluating impacts of CO_2 intrusion into an unconsolidated aquifer: I. Experimental data. International Journal of Greenhouse Gas Control 44, 323-333.

Lewicki, J.L., Birkholzer, J., Tsang, C.-F., 2006. Natural and industrial analogues for leakage of CO_2 from storage reservoirs: identification of features, events, and processes and lessons learned. Environmental Geology 52, 457.

Lions, J., Devau, N., de Lary, L., Dupraz, S., Parmentier, M., Gombert, P., Dictor, M.-C., 2014. Potential impacts of leakage from CO_2 geological storage on geochemical processes controlling fresh groundwater quality: A review. International Journal of Greenhouse Gas Control 22, 165-175.

Lofts, J., A. Zett, P. Clifford, Y. Li, R. Krahenbuhl and A. Seshia (2019). Three-Axis Borehole Gravity Logging for Reservoir Surveillance. SPE Middle East Oil and Gas Show and Conference. Manama, Bahrain, Society of Petroleum Engineers: 13.

Namhata, A., Zhang, L., Dilmore, R.M., Oladyshkin, S., Nakles, D.V., 2017. Modeling changes in pressure due to migration of fluids into the Above Zone Monitoring Interval of a geologic carbon storage site. International Journal of Greenhouse Gas Control 56, 30-42.

Nicol, A., Seebeck, H., Field, B., McNamara, D., Childs, C., Craig, J., Rolland, A., 2017. Fault Permeability and CO_2 Storage. Energy Procedia 114, 3229-3236.

Nind, C., J. MacQueen, P.D., Wasylechko, R., Chemam, M., Nackers, C., 2013. Gravilog: An update on the development and use of borehole gravity for mining exploration, ASEG Extended Abstracts 2013: 23rd Geophysical Conference, pp. 1-5.

Nooner, S.L., Eiken, O., Hermanrud, C., Sasagawa, G.S., Stenvold, T., Zumberge, M.A., 2007. Constraints on the in situ density of CO_2 within the Utsira formation from time-lapse seafloor gravity measurements. International Journal of Greenhouse Gas Control 1, 198-214.

Pollak, M.F., Bielicki, J.M., Dammel, J.A., Wilson, E.J., Fitts, J.P., Peters, C.A., 2013. The Leakage Impact Valuation (LIV) Method for Leakage from Geologic CO_2 Storage Reservoirs. Energy Procedia 37, 2819-2827.

Pruess, K., 2004. The TOUGH Codes--A Family of Simulation Tools for Multiphase Flow and Transport Processes in Permeable Media. Vadose Zone Journal, 3(3), 738-746.

Romanak, K.D., Bennett, P.C., Yang, C., Hovorka, S.D., 2012. Process-based approach to CO_2 leakage detection by vadose zone gas monitoring at geologic CO_2 storage sites. Geophys. Res. Lett. 39.

Telford, W.M., 1976. Applied geophysics. Cambridge University Press, London.

UBC-Geophysical Inversion Facility, 2017. GRAV3D Documentation, release 5.0, University of British Columbia.

US EPA, 2010. Federal Requirements Under the Underground Injection Control (UIC) Program for Carbon Dioxide (CO_2) Geologic Sequestration (GS) Wells; Final Rule. 76 FR 56982.

Van Camp, M., de Viron, O., Watlet, A., Meurers, B., Francis, O., Caudron, C., 2017. Geophysics From Terrestrial Time-Variable Gravity Measurements. Reviews of Geophysics 55, 938-992.

Wagoner, J., 2009. 3D Geologic Modeling of the Southern San Joaquin Basin for the Westcarb Kimberlina Demonstration Project- A Status Report, United States.

Wainwright, H., Finsterle, S., Zhou, Q., Birkholzer, J.T., 2013. Modeling the performance of large-scale CO_2 storage systems: A comparison of different sensitivity analysis methods. International Journal of Greenhouse Gas Control, 17, 189–205.

Wang, Z., Harbert, W.P., Dilmore, R.M., Huang, L., 2018. Modeling of time-lapse seismic monitoring using CO_2 leakage simulations for a model CO_2 storage site with realistic geology: Application in assessment of early leak-detection capabilities. International Journal of Greenhouse Gas Control 76, 39-52.

White, J.A., Foxall, W., 2016. Assessing induced seismicity risk at CO_2 storage projects: Recent progress and remaining challenges. International Journal of Greenhouse Gas Control 49, 413-424.

Wilkinson, M., Mouli-Castillo, J., Morgan, P., & Eid, R., 2017. Time-lapse gravity surveying as a monitoring tool for CO_2 storage. International Journal of Greenhouse Gas Control, 60 (Supplement C), 93-99.

Yang, C., Dai, Z., Romanak, K.D., Hovorka, S.D., Treviño, R.H., 2014a. Inverse Modeling of Water-Rock-CO_2 Batch Experiments: Potential Impacts on Groundwater Resources at Carbon Sequestration Sites. Environmental Science & Technology 48, 2798-2806.

Yang, C., Hovorka, S.D., Young, M.H., Trevino, R., 2014b. Geochemical sensitivity to CO_2 leakage: detection in potable aquifers at carbon sequestration sites. Greenhouse Gases: Science and Technology 4, 384-399.

Zhang, K., Wu, Y.S., Pruess, K., 2008. User’s Guide for TOUGH2-MP - A Massively Parallel Version of the TOUGH2 Code. Lawrence Berkeley National Laboratory, Berkeley, CA, USA.

Zhou, Q., and Birkholzer, J.T., 2011. On scale and magnitude of pressure build-up induced by large-scale geologic storage of CO_2. Greenhouse Gases: Science and Technology 1, 11-20.